

Coulomb universality

Leo Radzihovsky¹ and John Toner²

¹*Department of Physics and Center for Theory of Quantum Matter, University of Colorado, Boulder, CO 80309**

²*Department of Physics and Institute for Fundamental Science, University of Oregon, Eugene, OR 97403†*

(Dated: September 26, 2024)

Motivated by a number of realizations of long-range interacting systems, including ultra-cold atomic and molecular gases, we study a neutral plasma with power-law interactions *longer-ranged* than Coulombic. We find that beyond a crossover length, such interactions are universally screened down to a standard Coulomb form in all spatial dimensions. This implies, counter-intuitively, that in two dimensions and below, such a "super-Coulombic" gas is asymptotically Coulombically confining at low temperatures. At higher temperatures, the plasma undergoes a deconfining transition that in two dimensions is the same Kosterlitz-Thouless transition that occurs in a conventional Coulomb gas, but at an elevated temperature that we calculate. We also predict that in contrast, above two dimensions, even when naively the bare potential is confining, there is no confined phase of the plasma at any nonzero temperature. In addition, the super-Coulomb to Coulomb crossover is followed at longer length scales by an *unconventional* "Debye-Huckel" screening, which leads to faster-than-Coulombic, power-law decay of the screened potential, in contrast to the usual exponentially decaying Yukawa potential. Furthermore, we show that power-law potentials that fall off more rapidly than Coulomb are screened down to a shorter-ranged power-law, rather than an exponential Debye-Huckel Yukawa form. We expect these prediction to be testable in simulations, and hope they will inspire experimental studies in various platforms.

I. INTRODUCTION

A. Motivation

Recently there have been a number of experimental realizations of long-range interacting systems, particularly in ultra-cold atomic and molecular gases. These include pseudo-spin systems of dipolar-interacting molecular gases[1, 2], trapped ions[3] and Rydberg atoms[4]. Low-dimensional condensed matter surface systems coupled to a gapless, higher dimensional "bulk" also display long-range generalized elasticity[5–8], which lead to power-law interacting topological defects.

Motivated by these systems, here we study the behavior of a d -dimensional, long-range interacting, *neutral* plasma (in contrast to a single component charged gas[9]). The system is described by a classical Hamiltonian,

$$H = \frac{1}{2} \int_{\mathbf{r}, \mathbf{r}'} n(\mathbf{r}) U_0(\mathbf{r} - \mathbf{r}') n(\mathbf{r}') + E_c \sum_{\alpha} n_{\alpha}^2, \quad (1)$$

where we have defined $\int_{\mathbf{r}} \equiv \int d^d r$, with a "bare" long-range power-law interaction

$$U_0(\mathbf{r}) = -K(r/a)^{\omega}, \quad \omega = 2 - d + \sigma, \quad (2)$$

where a is a microscopic length scale.

We dub systems with $\sigma > 0$ "super-Coulombic" and $\sigma < 0$ "sub-Coulombic", because such interactions

are, respectively longer- and shorter-ranged than a d -dimensional Coulombic interaction. Here K , the constant interaction strength, satisfies $K\omega > 0$ (so as to ensure attraction [repulsion] of opposite [like] charges), and in equation (1) E_c is the "core" energy, determined by short-scale energetics. The charges $n(\mathbf{r})$ are quantized in the sense that

$$n(\mathbf{r}) = \sum_{\alpha} n_{\alpha} \delta^d(\mathbf{r} - \mathbf{r}_{\alpha}) \quad (3)$$

with integer charges n_{α} .

The Fourier transform of the interaction, computed in Appendix C is given by

$$U_0(\mathbf{q}) = C(\sigma, d) K / q^{2+\sigma}, \quad (4)$$

where $C(\sigma)$ is $O(a^{-\omega})$ function of σ (and of dimension of space d , argument that we have suppressed for simplicity). The precise value of $C(\sigma)$ is given in Appendix C, and is unimportant. All that matters is that it is finite for all σ in the range of interest $-2 < \sigma < 2$, that is, for interactions longer range than Coulombic, and the combination of $C(\sigma)K$ is always positive, when the bare interaction between opposite charges is attractive.

B. Results

Before turning to the analysis we first summarize our results. We find that the power-law interacting plasma exhibits qualitatively different behavior for $d > 2$, $d = 2$, and $d < 2$, that also depends on the signs of both σ and ω . As we will demonstrate, generically the potentials can exhibit quite novel (crossover) screening of two distinct types: (1) a power-law changing "dielectric" screening

* radzihov@colorado.edu

† jjt@uoregon.edu

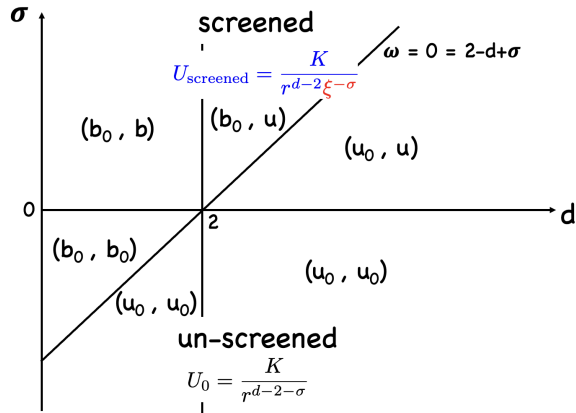


FIG. 1. Illustration of the distinct screening regimes of a super/sub-Coulombic potential, which depend on the signs of σ and ω , and on whether the spatial dimension d is less than, greater than, or equal to 2. Different regimes are labelled by the nature of the bare $U_0(r)$ (subscript 0) and screened $U_{\text{eff}}(r)$ potentials, with b and u denoting bound and unbound forms.

beyond a length which we will call ξ , and (2) an unconventional power-law “Debye-Huckel” screening beyond a length which we will call ξ_{DH} . The different behaviors and the regimes in which they hold are summarized in Fig. 1.

As illustrated there, for $\omega > 0$, at short scales the two-component plasma (described by the microscopic potential $U_0(r) \sim r^\omega$) behaves like a dielectric insulator with charges tightly bound into neutral dipoles. We denote this behavior by the symbol “ b_0 ”, which indicates that the bare potential is “binding”. Then for $\sigma > 0$, we find that, as illustrated in Fig.2, on intermediate length scales longer than the crossover (screening) length

$$\xi = a \left[y^{-2} \left(\frac{K}{k_B T} \right)^{\left(\frac{d+2}{\omega} \right) - 1} \right]^{1/\sigma} \times O(1), \quad (5)$$

(here $y \equiv e^{-\frac{E_c}{k_B T}}$ is the fugacity) a super-Coulombic ($\sigma > 0$) potential is *universally* “screened” down to a conventional ($\sigma = 0$) Coulomb potential, with a Fourier transform $U_{\text{eff}}(\mathbf{q}) \sim 1/q^2$. The resulting effective potential $-U_{\text{eff}}(\mathbf{r})$ between *opposite* charges in real space therefore crosses over from the growing bare potential $-U_0(\mathbf{r})$ given by (2) to a Coulombic, i.e., $U_{\text{eff}}(r) \propto r^{2-d}$ power-law. That is,

$$U_0(\mathbf{r}) = -K \left(\frac{r}{a} \right)^{2-d+\sigma} \xrightarrow[r \gg \xi]{d \neq 2} U_{\text{eff}}(\mathbf{r}) = -K \left(\frac{\xi}{a} \right)^\sigma \left(\frac{r}{a} \right)^{2-d} \quad (6)$$

As is clear from Fig. 1, what then happens to the potential at asymptotically long scales depends on the spatial dimension. For $d < 2$, the Coulomb power-law is “confining”; that is, the potential between opposite

charges goes to infinity as $r \rightarrow \infty$, which makes the Boltzmann weight for widely separated pairs vanish. Hence, oppositely charged pairs remain *bound*, even after the effect of dielectric screening is taken into account. We denote this by “ b ” (bound) in Fig. 1. Because the pairs remain tightly bound, this Coulombic power-law potential persists out to arbitrarily large distances. We emphasize that in this case, the long-distance limit of the potential is still a power law, albeit smaller than that of the bare potential, rather than an exponential decay. That is, the “screening” on these intermediate scales is more akin to the development of a non-zero dielectric constant (albeit length scale dependent and equivalently one that diverges as $q \rightarrow 0$) in an *insulating dielectric* medium, than it is to the familiar Debye-Huckel (DH) screening down to an exponentially decaying Yukawa potential.

On the other hand, for $d > 2$, the Coulomb power-law that appears for $r > \xi$ is no longer confining in the above-described sense, since it vanishes as $r \rightarrow \infty$. As a result, at nonzero temperature, for $r > \xi_{DH}$, where $\xi_{DH} > \xi$, the system will generically undergo a second, “Debye-Huckel” screening of the Coulomb potential. However, quite surprisingly, in contrast to a Coulombic conducting plasma, here the Debye-Huckel screening is *unconventional*, leading to an asymptotically *power-law* (rather than decaying exponential Yukawa) tail of the potential,

$$U_{\text{eff}}(\mathbf{r}) \approx \frac{C_{DH}}{r^{d+2+\sigma}}, \quad (7)$$

that decays faster than the Coulomb power-law $U_{\text{Coulomb}}(\mathbf{r}) \sim 1/r^{d-2}$ and (obviously) more slowly than the conventional exponential Yukawa screening one finds for Coulombic potentials. The precise expression for C_{DH} is given in equation (39) of section (IV A), and (C72) of Appendix C. Its precise value depends on parameters of the model (σ, K, E_c, \dots), as well as the spatial dimension d and $k_B T$. However, the *sign* of C_{DH} depends only on the spatial dimension d and the exponent σ . This sign is *negative* for all σ 's in the range $0 < \sigma < 1$ in $d = 1$ and $0 < \sigma < 2$ in $d = 2$ and $d = 3$. However, it becomes positive again for $2 < \sigma < 3$ in $d = 3$.

Recalling that $U_{\text{eff}}(\mathbf{r})$ is the interaction between *like* charges, this implies that the cases enumerated above in which $C_{DH} < 0$, there is *overscreening*, i.e., an attractive interaction tail between like charges.

Bare *confining* ($\omega > 0$) *sub-Coulombic* ($\sigma < 0$) potentials, which are shorter-ranged than Coulombic, remain *completely unscreened* at low temperatures. However, rather surprisingly, we find that the *non-confining* ($\omega < 0$) *sub-Coulombic* ($\sigma < 0$), bare potentials do Debye-Huckel screen, but they do so far less effectively than Coulombic potentials. Specifically, they only screen down to a *power-law* effective potential, identical to the DH power-law screening form for $\sigma > 0$, $d > 2$ given in Eq.(7). Although such $\sigma < 0$, $\omega < 0$ potentials decay faster than their bare form, they decay more slowly than both the exponential Yukawa screening one finds for Coulombic and the power-law (7) of super-Coulombic

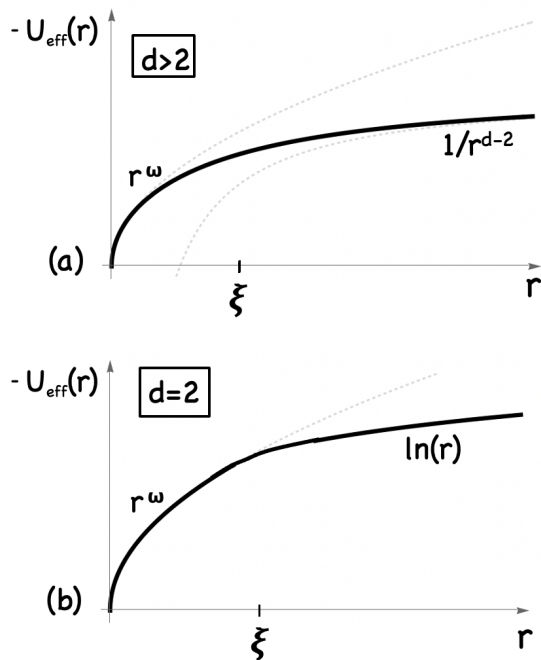


FIG. 2. Illustration of the dielectric-like screening of a super-Coulomb potential for $\omega > 0$ down to a conventional Coulomb potential beyond the crossover scale ξ given by equation (5). (a) shows the case $d > 2$ with a confining bare potential, $\omega > 0$ crossing over to the Coulomb non-confining potential, which approaches a non-zero constant (not indicated in the figure) as $-U_{\text{eff}}(r) \sim \text{const.} - 1/r^{d-2}$. Because such a decaying potential is non-binding, on scales longer than ξ_{DH} , the resulting conducting plasma will then undergo *unconventional* Debye-Huckel screening down to a more rapidly decaying *power-law* form (7) (not illustrated in the figure). In (b), the $d = 2$ crossover beyond ξ is to a logarithmically confining Coulomb form. As a result, opposite charges are bound into dipoles at low temperatures. However, the system undergoes a conventional KT transition[10] as temperature is increased, with an enhanced transition temperature, to a phase exhibiting *unconventional* Debye-Huckel *power-law* interactions, (rather than the conventional exponentially decaying Yukawa potential), as discussed in the manuscript.

potentials (since their σ is negative).

Finally, as illustrated in Fig. 2(b) for $d = 2$ and $\omega > 0$ and $\sigma > 0$, the screening is to a confining log-

arithmic form. Thus we strikingly predict a Kosterlitz-Thouless (KT) phase transition[10] in a system with a microscopically-power-law-confining potential (i.e., one with $\omega > 0$). This transition occurs at a temperature given in the large core energy limit $E_c \gg k_B T$ by,

$$k_B T_{KT} \approx \frac{\sigma E_c}{2 \ln\left(\frac{\sigma E_c}{K}\right)}. \quad (8)$$

We will demonstrate these results in two independent ways: (i) a mapping to a sine-Gordon theory, and (ii) a dielectric theory. These derivations are given in Sections II and III, respectively, with details of the analysis relegated to Appendices A and B. Reassuringly, the two approaches give perfectly consistent results. In Sec. IV E we will analyze the KT transition temperature for the $d = 2$ case. We will discuss the relation of the two-component power-law interacting gas to long-range exchanged XY model in Sec. V, and conclude in Sec. VI.

II. SINE-GORDON SCREENING

We begin with a derivation of above results using a dual sine-Gordon model description of the long-range interacting gas, defined by Hamiltonian in (1). To this end, we put the model (1) on a lattice:

$$H = \frac{1}{2} \sum_{\mathbf{r}, \mathbf{r}'} n_{\mathbf{r}} U_0(\mathbf{r} - \mathbf{r}') n_{\mathbf{r}'} + E_c \sum_{\mathbf{r}} n_{\mathbf{r}}^2, \quad (9)$$

where the sums run over the sites \mathbf{r}, \mathbf{r}' of a regular lattice, and the $n_{\mathbf{r}}$ are integers defined on those sites. The partition function for this model at temperature T is just the sum of the Boltzmann weight for this Hamiltonian over all configurations $\{n_{\mathbf{r}}\}$ of the integers $n_{\mathbf{r}}$ on the lattice:

$$Z = \sum_{\{n_{\mathbf{r}}\}} e^{-H[\{n_{\mathbf{r}}\}]/k_B T}. \quad (10)$$

We now follow the standard treatment[11] of the ordinary Coulomb gas by introducing a Hubbard-Stratonovich field $\theta_{\mathbf{r}}$ to mediate the long-range interaction. That is, we rewrite the partition function (10) as

$$Z = \sum_{\{n_{\mathbf{r}}\}} \prod_{\mathbf{r}} \left[\int d\theta_{\mathbf{r}} \right] \exp \left[-\frac{k_B T}{2C(\sigma)K} \int_{\mathbf{q}} q^{2+\sigma} |\theta_{\mathbf{q}}|^2 - \sum_{\mathbf{r}} \left(\frac{E_c}{k_B T} n_{\mathbf{r}}^2 - i\theta_{\mathbf{r}} n_{\mathbf{r}} \right) \right], \quad (11)$$

where $\theta_{\mathbf{q}}$ is simply the Fourier transform of $\theta_{\mathbf{r}}$. Performing the Gaussian integral over $\theta_{\mathbf{q}}$ in this expression is readily seen to recover the interaction (9) between charges in Fourier space of the original model.

Reorganizing the sums and products in (11) gives

$$Z = \prod_{\mathbf{r}} \left[\int d\theta_{\mathbf{r}} \right] e^{-\frac{1}{k_B T} \sum_{\mathbf{r}} V[\theta_{\mathbf{r}}] - \frac{\tilde{K}}{2k_B T} \int_{\mathbf{q}} q^{2+\sigma} |\theta_{\mathbf{q}}|^2}, \quad (12)$$

where the summation over *integer* charges $n_{\mathbf{r}}$ on each

lattice site \mathbf{r} gives the *periodic* "Villain potential" [12] of $\theta_{\mathbf{r}}$,

$$V[\theta_{\mathbf{r}}] \equiv -k_B T \ln \left[\sum_{n_{\mathbf{r}}=-\infty}^{\infty} e^{-\frac{E_c}{k_B T} n_{\mathbf{r}}^2 + i\theta_{\mathbf{r}} n_{\mathbf{r}}} \right], \quad (13)$$

and we have defined the "dual stiffness"

$$\tilde{K} \equiv \frac{(k_B T)^2}{C(\sigma)K}. \quad (14)$$

Note that $V[\theta_{\mathbf{r}}]$ is manifestly a periodic function of $\theta_{\mathbf{r}}$ with period 2π .

Going back to the continuum, the partition function (12) is then given by a path integral ($\int [d\theta(\mathbf{r})] \equiv \prod_{\mathbf{r}} \int [d\theta_{\mathbf{r}}]$) over the field $\theta(\mathbf{r})$, $Z = \int [d\theta(\mathbf{r})] e^{-\tilde{H}[\theta(\mathbf{r})]/k_B T}$, with the generalized dual *long-range* sine-Gordon model Hamiltonian, given by

$$\tilde{H} = \frac{1}{2} \tilde{K} \int_{\mathbf{q}} q^{2+\sigma} |\theta_{\mathbf{q}}|^2 - \sum_{n=1}^{\infty} g_n \int_{\mathbf{r}} \cos(n\theta(\mathbf{r})), \quad (15)$$

where the g_n 's are a^d times the expansion coefficients in the Fourier series for the periodic potential $-V[\theta(\mathbf{r})]$, with a^d the hypervolume of the unit cell of the lattice we introduced earlier. Because higher harmonics are always less relevant, and much smaller [11], we will focus on the first one, g_1 .

Indeed, it is straightforward to see that, for small "fugacity" $y \equiv e^{-\frac{E_c}{k_B T}} \ll 1$, the sum in (13) is dominated by the $n_{\mathbf{r}} = 0, \pm 1$ terms giving

$$V[\theta_{\mathbf{r}}] \approx -k_B T \ln \left[1 + 2y \cos(\theta_{\mathbf{r}}) \right] \approx -2k_B T y \cos(\theta_{\mathbf{r}}), \quad (16)$$

from which we can read off

$$g_1 \approx 2k_B T y a^{-d} = 2k_B T e^{-\frac{E_c}{k_B T}} a^{-d}, \quad (17)$$

where the factor of the inverse of the unit cell volume a^d arises, as mentioned earlier, from going over from the lattice to the continuum. By extending this argument to terms higher order in the fugacity y , one can show that, in the limit of small fugacity, the higher harmonics $g_{n>1} \propto y^n \propto e^{-\frac{nE_c}{k_B T}} \ll g_1$, as asserted earlier.

One might naively expect that the behavior of the model in two dimensions (2D) would differ significantly and qualitatively from that of the conventional-gradient-elasticity ($\sigma = 0$) sine-Gordon model. For $\sigma = 0$ in 2D, the cosine terms are "relevant", in the RG sense of changing the long-wavelength behavior of the system, for large stiffness \tilde{K} , which corresponds to high temperatures of the original model (1), and to the unbinding of charge dipoles [11]. In contrast, for our system, the "soft" $q^{2+\sigma}$ elasticity of the *long-range* sine-Gordon model (15) would naively appear to ensure that for $\sigma > 0$, the cosine nonlinearities are *always* – for *all* T and K – *irrelevant* for weak

g_n couplings. That is, the enhanced $\theta(\mathbf{r})$ fluctuations at long wavelengths always "average" away the weak cosine nonlinearities. In the context of a 2D XY model, this is simply a restatement in the dual language of the naive intuition that vortices would *always* be bound by a potential that is longer ranged than logarithmic.

However, our key and surprising discovery is that this naive conclusion is in fact incorrect. It is invalidated by universal screening of the long-range interaction $1/q^{2+\sigma}$ in (1), which reduces that interaction to the conventional Coulomb $1/q^2$ interaction, for all $\sigma > 0$.

This is easiest to see directly in the long-range sine-Gordon formulation (15) through a renormalization group (RG) analysis done perturbatively in the g_n 's. As we detail in the Appendix A, the renormalization group always generates a non-zero "spin-wave stiffness", $\frac{1}{2}\kappa(\nabla\theta)^2$ term in the sine-Gordon model, where $\kappa = O(g^2)$. At sufficiently long scales r – specifically for $r \gg \xi \sim g^{-2/\sigma}$, (a detailed expression for ξ is given in (19), and derived in the SM) – for the super-Coulombic case $\sigma > 0$, this dominates over the "soft" long-range "elasticity" (15) at small q , since $\tilde{K}q^{2+\sigma} \ll \kappa q^2$ for $q\xi \ll 1$. Reversing the above duality procedure, one can see that this gives an effective interaction between charges at these longer length scales that is the Fourier transform of $1/q^2$; i.e., the conventional Coulomb interaction $1/r^{d-2}$ in $d > 2$, and $\ln r$ in $d = 2$, as claimed in Eq. (6). This Coulombic interaction replaces the longer ranged $U_0(\mathbf{r})$ in (1) for scales longer than the crossover length ξ . In the Appendix A, we do this renormalization group calculation of both κ and the crossover length ξ in detail, and show that at long scales, the effective "spin-wave" stiffness κ is given by

$$\begin{aligned} \kappa &= k_B T \left(\frac{k_B T}{K} \right)^{(d+2)/\omega} a^{2-d} e^{-2E_c/k_B T} \times O(1), \\ &= \frac{(k_B T)^2 a^\omega}{K \xi^\sigma} \times O(1), \end{aligned} \quad (18)$$

with the crossover length

$$\xi = a \left[\left(\frac{K}{k_B T} \right)^{\left(\frac{d+2}{\omega}\right)-1} \left(\frac{1}{y^2} \right) \right]^{1/\sigma} \times O(1). \quad (19)$$

Undoing the duality procedure then implies that the effective screened interaction between charges at length scales much larger than the crossover length scale ξ is given by the conventional Coulomb one,

$$U_{\text{eff}}(\mathbf{r}) = \frac{K_{\text{Coulomb}}}{r^{d-2}}, \quad (20)$$

with the effective Coulombic coupling strength K_{Coulomb} given by

$$K_{\text{Coulomb}} = \frac{(k_B T)^2}{\kappa} = K a^{d-2} (\xi/a)^\sigma \times O(1). \quad (21)$$

In contrast, for a bare potential that is shorter-ranged than Coulombic ($\sigma < 0$), it is clear by inspecting the

Hamiltonian (15) that the $q^{2+\sigma}$ term will *always* dominate over the fluctuation generated q^2 term. As a result, the effective interaction $U_{\text{eff}}(r)$ between vortices retains its bare r^ω form.

III. DIELECTRIC SCREENING

A more familiar, although algebraically slightly more complicated argument for the above universal screening prediction is a complementary dielectric medium analysis of the long-range interaction (1).

This calculation is based on the observation that even tightly bounds pairs of charges create a "dipole" field at large distances. These tightly bound dipoles tend to align with an externally imposed field, in such a way as to cancel off the external field. This is the mechanism that generates a non-unit dielectric constant in a dielectric in-

ulator, as opposed to the Debye-Huckel screening down to a Yukawa potential that takes place in a conducting plasma of free charges.

As a result of these "induced" dipoles, the effective interaction between two unit test charges introduced to our system is given by:

$$U_{\text{eff}}(\mathbf{r}) = U_0(\mathbf{r}) + U_i(\mathbf{r}), \quad (22)$$

where the induced dipole potential at the point \mathbf{r} is given by

$$U_i(\mathbf{r}) = \sum_{\alpha} U_{d\alpha}(\mathbf{r} - \mathbf{r}_{\alpha}), \quad (23)$$

where $U_{d\alpha}(\mathbf{r})$ is the potential induced at point \mathbf{r} by a dipole at \mathbf{r}_{α} . For a pair of equal and opposite charges n_{α} (screening dipole constituents) separated from each other by \mathbf{v}_{α} , this is given by

$$U_{d\alpha}(\mathbf{r} - \mathbf{r}_{\alpha}) = n_{\alpha}[U_0(\mathbf{r} - \mathbf{r}_{\alpha}) - U_0(\mathbf{r} - \mathbf{r}_{\alpha} + \mathbf{v}_{\alpha})] \approx -n_{\alpha}\mathbf{v}_{\alpha} \cdot \nabla U_0(\mathbf{r} - \mathbf{r}_{\alpha}) \equiv -\mathbf{p}_{\alpha} \cdot \nabla U_0(\mathbf{r} - \mathbf{r}_{\alpha}) \quad (24)$$

where $\mathbf{p}_{\alpha} \equiv n_{\alpha}\mathbf{v}_{\alpha}$ is the dipole moment of the α 'th dipole. The induced potential $U_i(\mathbf{r})$ is thus given by

$$U_i(\mathbf{r}) = -\sum_{\alpha} \mathbf{p}_{\alpha} \cdot \nabla U_0(\mathbf{r} - \mathbf{r}_{\alpha}) = -\int_{\mathbf{r}'} \mathbf{p}(\mathbf{r}') \cdot \nabla U_0(\mathbf{r} - \mathbf{r}'), \quad (25)$$

where

$$\mathbf{p}(\mathbf{r}') \equiv \sum_{\alpha} \mathbf{p}_{\alpha} \delta^d(\mathbf{r}' - \mathbf{r}_{\alpha}) \quad (26)$$

is the local vectorial dipole density at \mathbf{r}' . Using this result in our expression (25) for the dipole potential, and putting the result in equation (22) leads to the total screened potential

$$U_{\text{eff}}(\mathbf{r}) = U_0(\mathbf{r}) - \int_{\mathbf{r}'} \mathbf{p}(\mathbf{r}') \cdot \nabla U_0(\mathbf{r} - \mathbf{r}'). \quad (27)$$

As in ordinary electrostatic dielectric theory, within linear response, the local dipole density $\mathbf{p}(\mathbf{r}')$ is proportional to the local "electric field":

$$\mathbf{p}(\mathbf{r}) = -\chi \nabla U_{\text{eff}}(\mathbf{r}), \quad (28)$$

where χ is the susceptibility. We calculate χ using the Boltzmann statistics of an isolated dipole in an external field in the Appendix B[13], with the result over a wide range of parameters[15] given by

$$\chi = \frac{y^2}{k_B T a^{d-2}} \left(\frac{k_B T}{K} \right)^{\left(\frac{d+2}{\omega} \right)} \times O(1). \quad (29)$$

The only feature of this result that we really need in the current discussion is that χ is non-zero, and finite. Using

the linear response relation (28) inside (27) gives,

$$U_{\text{eff}}(\mathbf{r}) = U_0(\mathbf{r}) + \chi \int_{\mathbf{r}'} \nabla' U_{\text{eff}}(\mathbf{r}') \cdot \nabla U_0(\mathbf{r} - \mathbf{r}'), \quad (30)$$

which can be straightforwardly solved in Fourier space, giving

$$U_{\text{eff}}(\mathbf{q}) = \frac{U_0(\mathbf{q})}{1 + \chi q^2 U_0(\mathbf{q})}. \quad (31)$$

Now, since, for $\sigma > 0$, $q^2 U_0(\mathbf{q}) = K a^{-\omega} / q^{\sigma}$ diverges as $q \rightarrow 0$, at sufficiently small q the term $\chi q^2 U_0(\mathbf{q})$ in the denominator of (31) dominates over the 1. More precisely, we see that this will occur for $q \ll \xi^{-1}$, where the screening length is given by

$$\xi = a^{\frac{\omega}{\sigma}} (K \chi)^{-\frac{1}{\sigma}} = a \left[\left(\frac{K}{k_B T} \right)^{\left(\frac{d+2}{\omega} \right) - 1} \left(\frac{1}{y^2} \right) \right]^{\frac{1}{\sigma}} \times O(1), \quad (32)$$

as advertised in (5) of the Introduction. Note from the second equality that this is precisely the same crossover length we found in the sine-Gordon approach, which is a non-trivial and reassuring check on the validity of both the sine-Gordon and this dielectric approach. Thus for $q \ll \xi^{-1}$ we obtain,

$$U_{\text{eff}}(\mathbf{q}) \approx \frac{1}{\chi q^2} \equiv \frac{K_{\text{Coulomb}}}{q^2}, \quad \text{for } q \ll \xi^{-1} \equiv a^{-\frac{\omega}{\sigma}} (\chi K)^{1/\sigma}, \quad (33)$$

where

$$K_{\text{Coulomb}} = \chi^{-1} = K a^{d-2} (\xi/a)^{\sigma} \times O(1), \quad (34)$$

Reassuringly, the sine-Gordon and the dielectric analyses agree in predicting that, quite generically, the screened potential asymptotically crosses over to the conventional Coulomb potential for *any* bare potential that is longer ranged than Coulombic ($\sigma > 0$), in *any* spatial dimension. Both calculations also give the same strength of that effective Coulomb potential.

Note also that if the bare interaction is itself Coulombic – that is, if $\sigma = 0$, the denominator in (31) is a finite constant larger than 1, and our result simply reduces to a Coulomb interaction reduced by the conventional dielectric constant of the medium. For a bare potential that is shorter-ranged than Coulombic ($\sigma < 0$), we also recover the result of the above in the sine-Gordon analysis, since, at small \mathbf{q} , the $\chi q^2 U_0(\mathbf{q})$ term in the denominator of (31) is $\ll 1$ (since in this case $U_0(\mathbf{q}) \ll 1/q^2$ as $\mathbf{q} \rightarrow \mathbf{0}$). As a result, at sufficiently small \mathbf{q} and large \mathbf{r} , the effective potential reduces to the bare potential.

IV. IMPLICATIONS FOR THE VARIOUS INTERACTION TYPES

As we now detail, the above results lead to a number of important implications for different cases of ω , σ and spatial dimension d , leading to two distinct “power-law dielectric” and “power-law Debye-Huckel” screening types, as summarized in Fig.1.

A. Screening of non-confining ($\omega < 0$) sub-Coulombic ($-2 < \sigma < 0$) potentials

We first observe that *sub-Coulombic* potentials (i.e., those with $\sigma < 0$) do not exhibit the dielectric-like screening we studied in Secs. II and III above. This can be seen in the sine-Gordon approach from the fact that the generated short-range κ elasticity is subdominant to the long-range \tilde{K} elasticity, and from the dielectric analysis based on Eq.(31), as discussed above.

However, for the non-confining case of $\omega < 0$, such *sub-Coulombic* $\sigma < 0$ potentials *do* in fact exhibit the analog of Debye-Huckel screening, but with a quite surprising *power-law* (rather than exponential) screened form. This can be derived from the sine-Gordon theory developed above by noting that, for $\omega < 0$, the cosine terms are *always* relevant, with eigenvalue d , which implies deconfinement of charges. This means that, at sufficiently long distances, $r \gg \xi_{DH}^- = (\tilde{K}/g)^{1/(2+\sigma)}$ (the “-” superscript is to distinguish this length from the analogous length ξ_{DH} for $\sigma > 0$, which we discuss below), the $-g \int_{\mathbf{r}} \cos \theta_{\mathbf{r}}$ always reduces to a non-zero effective “mass” g for the dual field $\theta_{\mathbf{r}}$ in (15). That is, the effective long-wavelength model becomes

$$\tilde{H} = \frac{1}{2} \int_{\mathbf{q}} (g + \tilde{K} q^{2+\sigma}) |\theta_{\mathbf{q}}|^2, \quad (35)$$

which in turn implies that the $\theta_{\mathbf{r}}$ correlations in Fourier space are given by

$$\langle |\theta_{\mathbf{q}}|^2 \rangle = \frac{k_B T}{g + \tilde{K} q^{2+\sigma}}. \quad (36)$$

By reversing our dual mapping onto the sine-Gordon theory, this implies that the Fourier transformed effective screened potential on wavenumber scales smaller than $(\xi_{DH}^-)^{-1}$ is given by

$$U_{\text{eff}}(\mathbf{q}) = \frac{(k_B T)^2}{g + \tilde{K} q^{2+\sigma}}. \quad (37)$$

If we expand $U_{\text{eff}}(\mathbf{q})$ for small \mathbf{q} , the first non-analytic term is $-\left(\frac{(k_B T)^2 \tilde{K}}{g^2}\right) q^{2+\sigma}$, which, as we show in Appendix C, implies

$$U_{\text{eff}}(\mathbf{r}) \approx \frac{C_{DH}}{r^{d+2+\sigma}}, \quad (38)$$

with

$$C_{DH} = G(\sigma, d) \left(\frac{(k_B T)^2 \tilde{K}}{g^2} \right), \quad (39)$$

where the dimensionless constant $G(\sigma, d)$ depends only on the spatial dimension d and the exponent σ . The precise, rather complicated expression for $G(\sigma, d)$ is given by equation (C72) of Appendix C. All we need to know here is that $G(\sigma, d)$ is finite and *positive* for all σ in the range $-2 < \sigma < 0$, and vanishes at $\sigma = 0$. This vanishing as $\sigma \rightarrow 0$ implies that there is no long-ranged power-law tail for Coulombic potentials, in agreement with the well-known result that Coulombic potentials are Debye-Huckel screened down to exponentially decaying Yukawa forms.

Our result (38) implies, rather surprisingly, that bare *sub-Coulombic* potentials with non-even integer $\sigma < 0$, which are shorter-ranged than Coulombic potentials, screen *less* effectively than those potentials on scales longer than ξ_{DH}^- , leading to effective *power-law* screened potentials at the longest distances. Obviously, such potentials are *longer*-ranged than the conventional exponentially screened Yukawa potential.

This result, taken together with our above result (38) for $-2 < \sigma < 0$, implies that the longest ranged effective potential (in the sense of decaying with the smallest power law with distance) occurs when $\sigma = -2$, in which case $U_{\text{eff}} \propto r^{-d}$.

B. Absence of screening for $\sigma < -2$

For $\sigma < -2$, the bare potential (1) falls into the class of potentials considered in part (C2d) of Appendix C, that is, its volume integral is finite, and, hence, its Fourier transform is finite as $\mathbf{q} \rightarrow \mathbf{0}$. More precisely, using equation (C71) of part (C2d) of Appendix C with

$\gamma = d - 2 - \sigma$, we see that the Fourier transform $U(\mathbf{q})$ of the bare potential can be written

$$U(\mathbf{q}) = U_a(\mathbf{q}) + A(\sigma, d)K a^{d-2-\sigma} q^{-(2+\sigma)}, \quad (40)$$

where $U_a(\mathbf{q})$ is an analytic function of \mathbf{q} which does not vanish as $\mathbf{q} \rightarrow 0$, and which depends only on q^2 , and $A(\sigma, d)$ is an unimportant constant. Note that for $\sigma < -2$ that we are considering here, the exponent $-(2+\sigma)$ of the explicitly displayed power of q in (40) is positive. Hence, this term is sub-dominant relative to the $U_a(\mathbf{q})$ term as $\mathbf{q} \rightarrow 0$ since that term does not vanish in that limit.

Now, when we perform the duality transformation on the plasma model (1), we obtain the sine-Gordon model Hamiltonian

$$\tilde{H} = \frac{1}{2} \int_{\mathbf{q}} G(\mathbf{q}) |\theta_{\mathbf{q}}|^2 - \sum_{n=1}^{\infty} g_n \int_{\mathbf{r}} \cos(n\theta(\mathbf{r})), \quad (41)$$

where we have defined

$$G(\mathbf{q}) \equiv \left(\frac{(k_B T)^2}{U_a(\mathbf{q}) + A(\sigma, d)K a^{d-2-\sigma} q^{-(2+\sigma)}} \right). \quad (42)$$

Since the $q^{-(2+\sigma)}$ term in this expression is subdominant relative to the $U_a(\mathbf{q})$ term as $\mathbf{q} \rightarrow 0$, if we expand $G(\mathbf{q})$ for small \mathbf{q} , we get

$$G(\mathbf{q}) = G_a(\mathbf{q}) + B(\sigma, d)q^{-(2+\sigma)}, \quad (43)$$

where $G_a(\mathbf{q})$ is an analytic function of \mathbf{q} which does not vanish as $\mathbf{q} \rightarrow 0$, and which depends only on q^2 , and $B(\sigma, d)$ is another unimportant constant.

Now consider the effect of renormalizing this model. Unlike the $\sigma > -2$ cases, the analytic structure of $G(\mathbf{q})$ will not change upon renormalization: it already has a non-zero ‘‘mass’’, so the mass generated by the cosine in (41) only adds to something that is already present. Likewise, generated q^2 terms will only add finite renormalizations to the q^2 terms already present in (43).

Hence, the analytic structure of the full sine-Gordon model (41) does not change upon renormalization. Thus, if we renormalize, and then undo our duality to obtain the effective potential, we will get an effective potential of *exactly* the same analytic structure as the bare potential. That is, it will still fall off like r^ω with $\omega = 2 - d + \sigma$. Namely, there is *no* screening in this case at all. Rather, the effect of the other charges in the system on the interaction of two test charges is more like the finite dielectric constant that occurs in Coulombic insulators: the *coefficient* of the long ranged tail of the interaction is changed by those other charges, but the power law of the interaction is not.

This result, taken together with our above result (38) for $-2 < \sigma < 0$, implies that the longest ranged effective potential (in the sense of decaying with the smallest power law with distance) occurs when $\sigma = -2$, in which case $U_{\text{eff}}(r) \propto r^{-d}$.

C. Screening for $d > 2$ super-Coulombic ($\sigma > 0$) potentials

In $d > 2$ the effect of the power-law dielectric-like screening we have derived in Secs. II and III is particularly striking for a bare potential that is *confining* on short scales, that is, one with $\omega > 0$. In this case, naively (i.e., ignoring the dielectric screening that we predict beyond ξ), one would expect that the charges would *always* be confined. However, in fact, as demonstrated above, on length scales beyond the crossover scale ξ the effective potential is screened down to a Coulomb potential. Since this potential *vanishes* as $\mathbf{r} \rightarrow \infty$ for $d > 2$, there can be no confinement of charges. Hence, we predict that the exact opposite of the naive expectation is true: charges are *never* confined, as is clear from Fig. (2b). Hence, there is only a single, deconfined phase in such a super-Coulombic neutral plasma in $d > 2$.

Furthermore, once the bare confining super-Coulombic potential ($\omega > 0$, $\sigma > 0$) screens down to a Coulomb potential, which is non-confining for $d > 2$, the two-component gas is a conducting plasma that is subject to a Debye-Huckel screening. In terms of the sine-Gordon model, this corresponds to the observation that for $d > 2$ the $-g \int_{\mathbf{r}} \cos(\theta_{\mathbf{r}})$ is always relevant (charges are always deconfined), reducing to a ‘‘massive’’ θ model,

$$\tilde{H}_{DH}^{\gg \xi} = \frac{1}{2} \int_{\mathbf{q}} \left[\tilde{K} q^{2+\sigma} + \kappa q^2 + g_R \right] |\theta_{\mathbf{q}}|^2, \quad (44)$$

with the effective coupling $g_R \equiv g e^{-c\xi^\omega}$ reduced by coarse-graining out to scales ξ (as detailed in Appendix A). Here c is a positive constant of order $a^{-\omega}$.

Thus, beyond the Debye-Huckel screening length $\xi_{DH} = (\kappa e^{c\xi^\omega}/g)^{1/2}$, the effective potential exhibits further deconfined plasma screening. One may naively think that it is possible to simply drop the $\tilde{K} q^{2+\sigma}$ term in (44), since for $\sigma > 0$ it is higher order in q than the generated κq^2 term. *If* it were possible to do so, one would then obtain the conventional exponentially short-ranged potential of the Yukawa type. However, as we will see below, beyond ξ_{DH} , the resulting real-space Debye-Huckel screened potential is generically (other than for an even integer σ) quite unconventional *power-law* in r , as advertised in Eq.(7) of the Introduction, rather than the decaying exponential Yukawa potential that one obtains for a conventional Coulomb plasma.

To see this somewhat surprising result, we first note that (44) gives,

$$\langle |\theta_{\mathbf{q}}|^2 \rangle = \frac{k_B T}{g_R + \kappa q^2 + \tilde{K} q^{2+\sigma}}, \quad (45)$$

that, by reversing our dual mapping onto the sine-Gordon theory, implies that the Fourier transformed effective screened potential $U_{\text{eff}}(\mathbf{q})$ on wavevectors smaller than ξ_{DH}^{-1} is given by

$$U_{\text{eff}}(\mathbf{q}) = \frac{(k_B T)^2}{g_R + \kappa q^2 + \tilde{K} q^{2+\sigma}}. \quad (46)$$

If we expand $U_{\text{eff}}(\mathbf{q})$ for small \mathbf{q} , the first non-analytic term is $-\left(\frac{(k_B T)^2 \tilde{K}}{g_R^2}\right) q^{2+\sigma}$, which, as we show in Appendix C, implies

$$U_{\text{eff}}(\mathbf{r}) \approx \frac{C_{DH}^R}{r^{d+2+\sigma}}, \quad (47)$$

with

$$C_{DH}^R = G(\sigma, d) \left(\frac{(k_B T)^2 \tilde{K}}{g_R^2} \right), \quad (48)$$

where the dimensionless constant $G(\sigma, d)$ depends only on the spatial dimension d and the exponent σ , and has the same form (C72) as for the sub-Coulombic case, but now with $\sigma > 0$. In $d = 3$ (which is obviously the only physically relevant case with $d > 2$), $G(\sigma, d)$, as can be seen from the plot Fig. (7), is positive for $2 < \sigma$, but *negative* for $0 < \sigma < 2$. Recalling that $U_{\text{eff}}(\mathbf{r})$ is defined as the interaction between *like* charges, we see that a positive $G(\sigma, d)$ implies an attractive interaction between opposite charges (like the bare interaction in (2)), while a *negative* $G(\sigma, d)$ implies a *repulsive* interaction between opposite charges. We call this phenomenon “overscreening”.

This overscreening only occurs when σ lies in the range $0 < \sigma < 2$, which corresponds in $d = 3$ to power-law potentials that fall off more slowly than a Coulombic $1/r$ potential (or grow), but do not grow as rapidly as a linear potential. That is, the power-law ω in (2) lies in the range $-1 < \omega < 1$.

The vanishing of $G(\sigma, d)$ as $\sigma \rightarrow 0$ implies that there is no long-ranged power-law tail for Coulombic potentials, in agreement with the well-known result that Coulombic potentials are Debye-Huckel screened down to exponentially decaying Yukawa forms.

The vanishing of $G(\sigma, d)$ as $\sigma \rightarrow 2$ in $d = 3$ is simply a consequence of the fact that the inverse Fourier transform of the bare potential is analytic in this case. It implies that there is no long-ranged power law tail to the effective interaction at long distances in this case. Instead, in this case, like the Coulomb case, we will have an exponentially decaying Yukawa potential at the longest distances.

D. Competition between dielectric and Debye-Huckel crossovers

Above we have discussed two qualitatively distinct types of screening: “dielectric-like” (discussed so far) screening that converts super-Coulombic potentials to Coulombic ones, and (unconventional) Debye-Huckel screening. Interestingly, both types of screening lead to asymptotical power-law potentials.

To summarize, we have considered four distinct cases: (i) for $\sigma < 0$, the dielectric screening is absent and only power-law Debye-Huckel screening takes place for $\omega < 0$; (ii) for $\sigma > 0$ and $d \leq 2$ (and concomitantly $\omega > 0$), at low temperatures the dielectric screening always takes

place first, since the gas is confining below a critical temperature, and Debye-Huckel screening only takes place above the deconfining phase transition temperature.

(iii) for $\sigma > 0$ and $d > 2$, both dielectric and Debye-Huckel screening take place. However, for $\omega > 0$, $-g \cos \theta$ is irrelevant on scales shorter than dielectric screening length ξ . As a result, the Debye-Huckel screening always takes place on scales *longer* than ξ , with ξ_{DH} always longer than ξ ;

(iv) in contrast to (iii), for $\sigma > 0$ and $d > 2$, but $\omega < 0$, $-g \cos \theta$ is relevant and both dielectric and Debye-Huckel screening can take place.

The last case (iv) exhibits a competition between the two types of screening, determined by the relative size of the corresponding screening lengths, ξ and ξ_{DH} . For (a) $\xi \ll \xi_{DH}$ the intermediate dielectric screening regime will survive up to length ξ , followed by Debye-Huckel screening beyond scale ξ_{DH} . Alternatively, for (b) $\xi \gg \xi_{DH}$, $-g \cos \theta$ is relevant and leads to a “mass” for θ on scales beyond ξ_{DH} . This thereby precludes the intermediate dielectric screening regime.

To determine the range of parameters for the regimes (iv) (a) and (iv) (b), we examine the ratio

$$\begin{aligned} \rho &\equiv \xi/\xi_{DH} \\ &= a \left[e^{\frac{2E_c}{k_B T}} \left(\frac{K}{k_B T} \right)^{\left(\frac{d+2}{\omega}\right)-1} \right]^{1/\sigma} \times (2k_B T e^{-\frac{E_c}{k_B T}} a^{-d}/\tilde{K})^{1/(2+\sigma)} \\ &= e^{\frac{\zeta_1 E_c}{k_B T}} \left(\frac{K}{k_B T} \right)^{\zeta_2}, \end{aligned} \quad (49)$$

where in the final equality, we have used equation (14) to rewrite \tilde{K} in terms of the original interaction strength K of the bare potential, and ignored factors of $O(1)$. We have also in the final equality defined

$$\zeta_1 \equiv \frac{4 + \sigma}{\sigma(2 + \sigma)}, \quad \zeta_2 \equiv \frac{2(1 + \sigma)}{\sigma(2 + \sigma)}. \quad (50)$$

Note that both $\zeta_{1,2} > 0$, since we are considering $\sigma > 0$ here.

Clearly, for low temperatures, specifically $k_B T \ll E_c$, the ratio ρ gets very large, and, hence, there is no intermediate dielectric regime. Instead, one crosses over directly from the bare interaction to the anomalous (power-law) Debye-Huckel screened one.

As we raise the temperature into the regime $k_B T \gtrsim E_c$ and $k_B T \gg K$, the ratio $\rho \ll 1$, and we will have an intermediate dielectric regime. To say this in another way, with increasing distance r , the interaction will first cross over from the bare interaction to a d -dimensional Coulomb interaction r^{2-d} , and then, at a much larger length scale ξ_{DH} , cross over to the unconventional (power-law) Debye-Huckel screened interaction (7).

E. Kosterlitz-Thouless transition in $d = 2$

The other important implication of the screening predicted above is in two dimensions. For a gas interacting with a bare confining potential, (i.e., $\omega > 0$), one might naively again expect that charges are always bound. In contrast, what we actually predict is screening to a logarithmic potential, as illustrated in Fig.(2a), beyond the crossover scale ξ in Eq.(5). This implies that such a gas will therefore undergo a conventional Kosterlitz-Thouless unbinding phase transition at $k_B T_{KT}/K_{\text{Coulomb}}(T_{KT}) = 1/4$ [10]. Utilizing our expression (34) for K_{Coulomb} , and setting $d = 2$ (i.e., $\omega = \sigma$), we see that this implies the KT transition temperature for a super-Coulomb gas obeys

$$\begin{aligned} k_B T_{KT} &= K \left(\frac{\xi(T_{KT})}{a} \right)^\sigma \times O(1), \\ &= \frac{k_B T_{KT}}{y^2} \left(\frac{K}{k_B T_{KT}} \right)^{\frac{4}{\sigma}} \times O(1) \\ &= \frac{k_B T_{KT}}{4} \left(\frac{K}{k_B T_{KT}} \right)^{\frac{4}{\sigma}} e^{2E_c/k_B T_{KT}} \times O(1). \end{aligned} \quad (51)$$

The solution of this equation for T_{KT} is

$$k_B T_{KT} = \frac{\sigma E_c}{2W_0 \left(\frac{\sigma E_c}{K} \times O(1) \right)}, \quad (53)$$

where $W_0(u)$ is the first branch of the Lambert W function[16]. Since all of our calculations have assumed a low charge density, which requires $y = e^{-E_c/k_B T} \ll 1$, which in turn implies $E_c/k_B T \gg 1$, we can use the asymptotic expression[16] for the Lambert W function W_0 for large argument to simplify (53) to

$$k_B T_{KT} \approx \frac{\sigma E_c}{2 \ln \left(\frac{\sigma E_c}{K} \right)}. \quad (54)$$

From this solution, it is clear that at least one bit of intuition about the effect of increasing the range of the potential (i.e., increasing σ) is correct: as we increase σ for fixed core energy E_c and interaction strength K , the Kosterlitz-Thouless transition temperature T_{KT} grows. Specifically, it grows roughly linearly with σ , up to the extremely weak logarithmic dependence on σ in the denominator of (54). However, the most important point is that it remains finite, and that *all* super-Coulombic potentials in 2d undergo an unbinding transition in the same Kosterlitz-Thouless universality class as Coulombic (i.e., logarithmic) potentials.

Above this Kosterlitz-Thouless transition temperature, the charges are unbound, and, hence, the unconventional (power-law) Debye-Huckel screening we discussed in the previous subsection for the unconfined super-Coulombic case will also take place in the unbound phase. Since here we are in $d = 2$, the result (38) becomes

$$U_{\text{eff}}(\mathbf{r}) \approx \frac{C_{DH}^R}{r^{4+\sigma}}. \quad (55)$$

The interaction strength C_{DH}^R is no longer given by (48), however, since all parameters will be renormalized by critical fluctuations near the Kosterlitz-Thouless transition. We defer a calculation of the critical behavior of this constant to a future publication.

F. Unbinding transition for $d < 2$

For $d < 2$, the Coulomb potential to which super-Coulombic bare potentials ($\sigma > 0$) dielectrically screen is binding (that is, it still grows with distance without bound like r^{2-d}). Furthermore, *sub-Coulombic* potentials ($\sigma < 0$), are dielectrically unscreened, and, when $\omega > 0$ (which can only occur in $d = 1$), are also binding. For $\sigma > 0$ (super-Coulombic) potentials in $d = 1$, the large distance behavior of the plasma (that is, its behavior on length scales $r > \xi$) is that of a plasma with linear ($U(r) \propto r$) interactions, while for $\sigma < 0$ (sub-Coulombic) potentials, $U(r) \propto r^\omega$ with $0 < \omega < 1$. Such $d = 1$ systems have been considered by Kosterlitz[17], who showed that, while charges are bound at low temperatures, there is an unbinding transition at a temperature T_c , above which the system is screened. We can reproduce this results using our sine-Gordon approach.

This transition in $d = 1$ is of a fairly conventional type. In particular, it has a finite correlation length exponent. That is, the correlation length $\xi_{\text{deconfine}}$ (which above T_c is the screening length) diverges according to

$$\xi_{\text{deconfine}} \propto |T - T_c|^{-\nu}, \quad (56)$$

in contrast to the exponential divergence of the correlation length at the Kosterlitz-Thouless transition[10]. For small ω , the exponent ν is given by[17]

$$\nu = \frac{1}{\sqrt{2\omega}}. \quad (57)$$

For super-Coulombic ($\sigma > 0$) potentials, the interaction screens down to Coulombic, which in $d = 1$ is characterized by an effective $\omega = 1$. Although for such large ω we lose quantitative control of ν , we expect that the power-law divergence of $\xi_{\text{deconfine}}$ in (56) remains valid, with a $\nu(\omega)$, which is universal in the sense of depending only on ν .

As with the Kosterlitz-Thouless transition of the previous subsection, here too, above the unbinding transition T_c the charges are in a plasma phase that will exhibit the unconventional power-law Debye-Huckel screening, Eq. (38), we derived in previous subsection for the unconfined super-Coulombic case.

V. LONG-RANGED XY MODELS

As noted in the Introduction, a significant motivation for our work was originally driven by recent experimental realizations of spin systems with power-law exchange,

such as dipolar ultra-cold atomic, ionic and molecular gases. One may then expect that screening of a super-Coulomb vortex gas will correspondingly lead to a modification of the power-law exchange of the 2D XY model. In this section we critically examine this expectation and demonstrate that it is *not* realized.

A. Failure of mapping to the super-Coulombic vortex gas

Based on the mapping of the 2D XY model onto a Coulomb gas of vortices[10], one might be tempted to naively conclude that our above screening results could be applied to a 2D XY model with long-range exchange interactions – that is, to a model in which unit length two-component "spins" live on a two-dimensional lattice whose sites are labelled by \mathbf{r} . The classical Hamiltonian for such a system is:

$$H = - \sum_{\mathbf{r}, \mathbf{r}'} J_{\mathbf{r}, \mathbf{r}'} \mathbf{S}_{\mathbf{r}} \cdot \mathbf{S}_{\mathbf{r}'} = - \sum_{\mathbf{r}, \mathbf{r}'} J_{\mathbf{r}, \mathbf{r}'} \cos[\phi_{\mathbf{r}} - \phi_{\mathbf{r}'}], \quad (58)$$

with the exchange coupling falling off algebraically with distance:

$$J_{\mathbf{r}, \mathbf{r}'} = J_0 \left(\frac{a}{|\mathbf{r} - \mathbf{r}'|} \right)^{4-\sigma}, \quad (59)$$

where the length a is a lattice constant. Our choice of the definition of σ in the power-law exponent $\alpha \equiv 4 - \sigma$ ($= 2 + d - \sigma$ in d -dimensions, that differs from others in the literature e.g., $\alpha = d + \sigma_F$ [19, 20]; see Appendix D) is motivated by our definition of σ in (2) and (4), as will become clear below.[18]

As famously shown by Kosterlitz and Thouless[10], the *short-ranged* XY model can be mapped onto a Coulomb gas of vortices by Taylor-expanding the cosine in (58) to quadratic order, going to the continuum, and by including vortex topological defects by writing

$$\phi(\mathbf{r}) = \sum_{\alpha} n_{\alpha} \phi^{\text{vortex}}(\mathbf{r} - \mathbf{r}_{\alpha}), \quad (60)$$

where we have defined

$$\phi^{\text{vortex}}(\mathbf{r}) = \arctan(y/x). \quad (61)$$

Naively applying the same reasoning to the *long-ranged* XY model, (58) one would (erroneously, as we will see below) conclude that the resulting vortex gas would map onto the super-Coulombic plasma (1) which we analyzed above, with the value of σ in (1) given by the σ of (59). If this were correct, then the universal screening result (33) would predict that at scales longer than the crossover-to-Coulomb interaction length, ξ , such a long-ranged XY model would reduce to the conventional, short-ranged XY model, and in 2D would be expected to undergo a Kosterlitz-Thouless phase transition.[10]

However, in fact, we know from the seminal work of Fisher et. al.[19] that the transition in a long-ranged 2D XY model is clearly *not* of the Kosterlitz – Thouless type. That paper (which we review in Appendix D) studied the complementary long-ranged Ginzburg-Landau $|\psi|^4$ model, in which the angle ϕ in (58) is the complex phase of the "soft spin" $\psi(\mathbf{r}) \sim e^{i\phi}$. This model faithfully includes vortex and spin-wave degrees of freedom.

The most dramatic difference between the KT and the transition found in Ref.19 is that the low-temperature phase has long-ranged ferromagnetic order, while the low-temperature Kosterlitz-Thouless phase has only quasi-long-ranged order. Almost as dramatic a difference is Fisher et. al.'s result that the ferromagnetic correlation length in high temperature phase diverges algebraically as the transition is approached from above, while it diverges exponentially at the KT transition[10]. Thus, Fisher et. al.'s[19] results (which can be tested for $\sigma = 1$ in the experimental system of Chen et. al.,[4]) therefore indicate a failure of the naive mapping of the long-ranged XY model onto a super-Coulombic vortex plasma (which we have shown above *does* have a KT transition in 2D).

It is natural to ask why the mapping of the long-ranged XY model to a gas of super-Coulombic vortices fails. The reason is the following: It is clear that in a *long-ranged* XY model, the energy is dominated by the interaction between spins that are far apart, for which, in the presence of vortices, the difference $|\phi_{\mathbf{r}} - \phi_{\mathbf{r}'}|$ is large, of order 2π . This therefore precludes the quadratic Taylor approximation of the cosine in (58) and therefore thwarts the naive mapping onto a quadratic Hamiltonian in $\phi_{\mathbf{r}}$ and by extension onto the super-Coulombic pairwise interacting model (1).

B. Vortex-free harmonic model

The lack of screening in the long-ranged XY model suggests that in the long-range ordered phase[19], vortices (expected to be tightly confined in the ordered phase) may be neglected. Therefore, the spin-wave theory, obtained by expanding the model (58) for small spin-waves $\phi_{\mathbf{r}} - \phi_{\mathbf{r}'}$ to quadratic order, with the crucial implicit constraint of no vortices in ϕ_r , is expected to be accurately described by the continuum Hamiltonian,

$$\begin{aligned} H &\approx \frac{1}{2} J_0 a^{-\sigma} \int_{\mathbf{r}, \mathbf{r}'} \left(\frac{1}{|\mathbf{r} - \mathbf{r}'|} \right)^{4-\sigma} [\phi(\mathbf{r}) - \phi(\mathbf{r}')]^2, \quad (62) \\ &\approx \frac{1}{2} K a^{-\sigma} \int_{\mathbf{q}} q^{2-\sigma} |\phi_{\mathbf{q}}|^2 \equiv \frac{1}{2} \int_{\mathbf{q}} \hat{K}(\mathbf{q}) q^2 |\phi_{\mathbf{q}}|^2. \quad (63) \end{aligned}$$

In the second line we defined $K \equiv C(\sigma)J_0$, with $C(\sigma) = \frac{8 \cos(\frac{\pi\sigma}{2}) \Gamma(\sigma) \Gamma^2(\frac{3-\sigma}{2})}{2^{\sigma} (2-\sigma) (1-\sigma) \Gamma(3-\sigma)}$ an $O(1)$ numerical factor. In the last equality we have defined the strongly wavevector-

dependent “spin-wave stiffness”

$$\hat{K}(\mathbf{q}) \equiv \frac{2J_0}{a^\sigma q^2} \int_{\mathbf{r}} \frac{1 - \cos(\mathbf{q} \cdot \mathbf{r})}{r^{4-\sigma}} \approx_{qa \ll 1} \frac{K}{(qa)^\sigma}, \quad (64)$$

which diverges as $\mathbf{q} \rightarrow \mathbf{0}$. We note that for the physically most relevant case of “dipolar” exchange,[1–4] $\sigma = 1$ and the dispersion in (63) is $\propto |q|$, with $C(1) = 2\pi$.

In this harmonic approximation, fluctuations of $\phi_{\mathbf{r}}$ within the ordered state are given by a simple Gaussian integral (or, equivalently, the equipartition theorem) with the Hamiltonian (63),

$$\begin{aligned} \langle \phi^2(\mathbf{r}) \rangle &= \int \frac{d^2q}{(2\pi)^2} \frac{k_B T}{\hat{K}(\mathbf{q}) q^2} = a^\sigma \int \frac{d^2q}{(2\pi)^2} \frac{k_B T}{K q^{2-\sigma}}, \quad (65) \\ &= \frac{k_B T}{2\pi\sigma K}, \quad (66) \end{aligned}$$

where we have used $1/a$ as the ultraviolet cutoff on the $\int d^2q$, and, for $\sigma > 0$ in the thermodynamic limit, $L \rightarrow \infty$, neglected finite size corrections which are smaller by a factor of $(a/L)^\sigma$. Thus, for long-range exchange – i.e., $\sigma > 0$ – we find that ϕ_{rms} is finite and system-size L -independent in the thermodynamic limit. This is clearly a reflection of the stabilizing effect of long-range interactions, with an effective exchange coupling $\hat{K}(q) \sim q^{-\sigma}$ that diverges at long length scales. It is consistent with the 2D long-range order and nonzero magnetization $\langle \mathbf{S}_{\mathbf{r}} \rangle$ at low temperatures found by Fisher et., al.[19] in their complementary “soft spin” description, and recently observed in two-dimensional Rydberg arrays.[4]

The ordered phase is also characterized by a nontrivial longitudinal susceptibility $\chi(h)$ for the response of the magnetization $M(h) = |\langle \mathbf{S}_{\mathbf{r}} \rangle|$ to an applied field h . Perturbing the zero-field Hamiltonian H with $-h \int_{\mathbf{r}} \mathbf{h} \cdot \mathbf{S}_{\mathbf{r}}$ gives $H_h = H - h \int_{\mathbf{r}} \cos(\phi(\mathbf{r}))$. In the ordered low- T phase, this gives for the magnetization

$$\begin{aligned} M(h) &= |\langle \mathbf{S}_{\mathbf{r}} \rangle| = \langle \cos(\phi(\mathbf{r})) \rangle \approx 1 - \frac{\langle \phi^2(\mathbf{r}) \rangle}{2} \\ &= 1 - \int \frac{d^2q}{(2\pi)^2} \frac{k_B T}{[K_0 a^{-\sigma} q^{2-\sigma} + h]}. \quad (67) \end{aligned}$$

The differential susceptibility $\chi(h)$ at small h can now be determined by differentiating (67):

$$\begin{aligned} \chi(h) &\equiv \left(\frac{\partial M}{\partial h} \right)_T = \int \frac{d^2q}{(2\pi)^2} \frac{k_B T}{[K_0 a^{-\sigma} q^{2-\sigma} + h]^2}, \\ &\approx \begin{cases} h^{-\mu}, & \text{for } 0 < \sigma < 1, \\ \frac{k_B T a^2}{2\pi K_0^2} \ln \left(\frac{K_0}{a^2 h} \right), & \text{for } \sigma = 1, \\ \chi_0, & \text{for } 1 < \sigma < 2, \end{cases} \quad (68) \end{aligned}$$

where we have defined the exponent

$$\mu \equiv 2 \left(\frac{1-\sigma}{2-\sigma} \right), \quad \text{for } 0 < \sigma < 1, \quad (69)$$

and χ_0 is a finite constant.

The qualitative distinction between the cases of $0 < \sigma \leq 1$ and $1 < \sigma < 2$ comes from the infrared divergence and convergence of the integral for $h = 0$ in (68), respectively, which correspondingly result in a divergent and finite susceptibility for $h \rightarrow 0$. The former case for $0 < \sigma < 1$ corresponds to a *sublinear* longitudinal magnetization response,

$$M(h) - M(0) \propto h^{\sigma/(2-\sigma)}. \quad (70)$$

For the case $\sigma = 1$, as in the experiments of Bakr et. al.[2], we get a logarithmic correction to the usual linear susceptibility, which is explicitly displayed in the middle line after the brackets in equation (68), while for $\sigma > 1$, the linear susceptibility is finite.

VI. RESULTS AND CONCLUSION

Motivated by the increasing number of experiments on long-ranged interacting systems, we have studied two-component power-law interacting super-Coulombic gases. We derived in complementary ways – via coarse-graining a sine-Gordon model and dielectric medium analyses – the screened inter-charge potential for such systems. Our key striking finding is that dipole screening universally leads to the standard $1/q^2$ Coulomb interaction, independent of the bare potential, as long as it is longer ranged than Coulombic. Along with a number of regimes summarized in Fig. 1, we also showed that, in contrast to naive expectations based on its short-ranged counterpart, the 2D long-ranged XY model is, in fact, *not* related to the super-Coulombic gas of vortices. It therefore is *not* screened down to a short-ranged XY model. Instead, it exhibits long-range ferromagnetic order with power-law bound vortices at low T , and does *not* undergo a Kosterlitz-Thouless transition.

We close by noting that the dielectric screening analysis is generic and dimension independent. It is intriguing to speculate that this screening mechanism may explain the ubiquity of Coulombic potentials in nature.

Note Added: After this work was completed (with the key result obtained over 34 years ago!) and in the long and delayed process of being written up, we learned of a recent interesting paper, arXiv:2209.11810, Journal of High Energy Physics, 2023(2), 1-25 (2022), *Villain model with long-range couplings* by Guido Giachetti, Nicolo Defenu, Stefano Ruffo, and Andrea Trombettoni.[21] There is overlap of our results with those found in this nice work, although ours has a somewhat broader scope.

In a separate development, we recently learned of an interesting paper by Igor Herbut and Babak Seradjeh[22] who study the question we address, but in a very specific setting of a magnetic monopole gas in QED-3, and argue that screening down to Coulomb interaction ensures instability of the state to deconfinement of monopoles and concomitant confinement of fermions.

Acknowledgments. We thank Waseem Bakr for discussions and the motivating experimental references. LR acknowledges support by the Simons Investigator Award from The James Simons Foundation. LR also thanks The Kavli Institute for Theoretical Physics for hospitality and its participants for discussions (especially Nicolo Defenu and co-authors of reference [21]) during the workshop "Exploring Non-equilibrium Long-range Quantum Matter", supported by the National Science Foundation under Grant No. NSF PHY-1748958 and PHY-2309135. JT thanks the IBM Research Almaden Lab for their hospitality during a summer 1990 visit during which this work was initiated, and the Max-Planck-Institut für Physik Komplexer Systeme (MPIPKS), Dresden, Germany, for their support and hospitality during a visit at which a portion of the writing of this paper was done.

Appendix A: Coarse-graining of a "soft" sine-Gordon model

Here we present the details of the renormalization group (RG) analysis of the "soft" sine-Gordon model (15), to prove our claim that the super-Coulombic 2D vortex gas is universally screened to a Coulombic interaction.

We begin by writing the sine-Gordon Hamiltonian (15) of the main text as

$$H_{SG} = H_0 + H_g, \quad (\text{A1})$$

where $\int \prod_{\mathbf{q}} d\theta_{\mathbf{q}}^>$ denotes an integral over *only* the fast degrees of freedom $\theta_{\mathbf{q}}^>$, and the symbol $\langle \dots \rangle_0^>$ denotes an average of \dots over those fast modes using *only* the Boltzmann weight $Z_0^{-1} e^{-\beta H_0[\theta_{\mathbf{r}}^>]}$ for the purely quadratic part of the Hamiltonian. Since this Hamiltonian is quadratic, these averages are straightforward to evaluate, being averages over a purely Gaussian distribution.

As we will see below, this quadratic part of the Hamiltonian will be drastically modified by the generation of the $\frac{1}{2}\kappa \int_{\mathbf{r}} (\nabla\theta)^2$ term, which will eventually, after a sufficient amount of renormalization group "time", come to dominate over the \tilde{K} term given above. In the discussion that follows, we will initially ignore the effect of this generated term on the quadratic Hamiltonian, and then we will discuss when this assumption ceases to be valid. The point at which that fails gives us the crossover length ξ between the super-Coulombic and Coulombic interactions.

The next step of the RG is (purely for convenience) to rescale lengths so as to restore the ultraviolet cutoff to its original value. The rescaling of wavevectors that

where

$$H_0 = \frac{1}{2} \tilde{K} \int_{\mathbf{q}} q^{2+\sigma} |\theta_{\mathbf{q}}|^2 \quad (\text{A2})$$

is the quadratic part of the Hamiltonian, while

$$H_g = -g \int_{\mathbf{r}} \cos(\theta_{\mathbf{r}}) \quad (\text{A3})$$

is the non-trivial part. Note that in (A3) we have kept only the lowest harmonic in the Fourier series in (15), and have defined $g \equiv g_1$

The RG[11] starts by separating the field $\theta_{\mathbf{r}} = \theta_{\mathbf{r}}^> + \theta_{\mathbf{r}}^<$ into "fast" and "slow" components $\theta_{\mathbf{r}}^>$ and $\theta_{\mathbf{r}}^<$, where the "fast" component $\theta_{\mathbf{r}}^>$ only has support in the "shell" of Fourier space $b^{-1}\Lambda \leq |\mathbf{q}| \leq \Lambda$, where Λ is an "ultra-violet cutoff", while the "slow" component $\theta_{\mathbf{r}}^<$ has support in the "core" $0 \leq |\mathbf{q}| \leq b^{-1}\Lambda$. Here Λ is of order the inverse lattice constant a^{-1} in a lattice model, and for continuum models comparable to the microscopic length scale on which our "charges" begin to show structure. Here b is an arbitrary rescaling factor. Later, to derive *differential* recursion relations, we will take $b = e^{d\ell}$ to be close to 1, with $d\ell \ll 1$.

We then derive an "intermediate" Hamiltonian $H_I(\theta^<)$ for the slow degrees of freedom $\theta^<$ by integrating the Boltzmann weight $Z^{-1} e^{-\beta H[\theta_{\mathbf{r}}^<, \theta_{\mathbf{r}}^>]}$ over the "fast" degrees of freedom $\theta_{\mathbf{r}}^>$, with $\beta \equiv 1/k_B T$. That is, we write

$$Z_I^{-1} e^{-\beta H_I[\theta_{\mathbf{r}}^<]} = Z^{-1} \int \prod_{\mathbf{q}} d\theta_{\mathbf{q}}^> e^{-\beta H[\theta_{\mathbf{r}}^<, \theta_{\mathbf{r}}^>]} = Z_0 Z^{-1} e^{-\beta H_0[\theta_{\mathbf{r}}^<]} \langle e^{-\beta H_g[\theta_{\mathbf{r}}^<, \theta_{\mathbf{r}}^>]} \rangle_0^>, \quad (\text{A4})$$

accomplishes this is, obviously, the change of variable

$$\mathbf{q} = b^{-1} \mathbf{q}'. \quad (\text{A5})$$

Due to the inverse relation between wavevectors \mathbf{q} and real space coordinates \mathbf{r} , this implies the opposite scaling of coordinates:

$$\mathbf{r} = b \mathbf{r}'. \quad (\text{A6})$$

We choose *not* to rescale the real-space field $\theta_{\mathbf{r}}$, in order to keep the coefficient of $\theta_{\mathbf{r}}$ in the the argument of $\cos(\theta_{\mathbf{r}})$ equal to 1, i.e., to keep the periodicity fixed at 2π , corresponding to discrete integer charges of the super-Coulomb gas. The renormalization group now proceeds by repetition of the above three RG steps (separating into fast and slow fields, averaging over the fast fields, and rescaling).

We perform the averaging over $\theta_{\mathbf{r}}^>$ perturbatively in $H_g = -g \int_{\mathbf{r}} \cos \theta_{\mathbf{r}}$. A standard second-order perturbation analysis gives for the change δH in the effective Hamil-

tonian for the remaining slow fields:

$$\delta H = \langle H_g \rangle_{0>} - \frac{\beta}{2} \langle H_g^2 \rangle_{0>}^c + \dots, \quad (\text{A7})$$

The rescaling step of the RG gives,

$$\tilde{K}(b) = \tilde{K} b^{-\omega}, \quad \text{with } \omega = 2 - d + \sigma. \quad (\text{A8})$$

This relation is *exact*, since \tilde{K} gets no corrections from the perturbative coarse-graining, due to the non-analytic, $q^{2+\sigma}$ form of the \tilde{K} term in (A2).

The leading-order coarse-graining correction to the coupling g comes from the first term in (A7), which gives

$$\begin{aligned} \delta H = \langle H_g \rangle_0^> &= -g \int_{\mathbf{r}} \langle \cos(\theta_{\mathbf{r}}^< + \theta_{\mathbf{r}}^>) \rangle_0^> \\ &= -g e^{-\frac{1}{2} \langle (\theta_{\mathbf{r}}^>)^2 \rangle_0^>} \int_{\mathbf{r}} \cos \theta_{\mathbf{r}}^<, \end{aligned} \quad (\text{A9})$$

where the second equality follows from writing the cosine in terms of complex exponentials, and then using the fact that, for a zero-mean, Gaussian field $\theta_{>}$ satisfies,

$$\langle e^{i\theta} \rangle = e^{-\frac{1}{2} \langle \theta^2 \rangle}. \quad (\text{A10})$$

This then gives the transformation of g under the RG,

$$\begin{aligned} g_R &= g b^d e^{-\frac{1}{2} G^>(\mathbf{0})} \\ &\approx g b^d \exp(-S_d(\ln b) k_B T / [2(2\pi)^d \tilde{K} \Lambda^\omega]) \end{aligned} \quad (\text{A11})$$

where the b^d factor comes from the length rescaling in $\int d^d r$. In (A12), we have defined the momentum-shell correlator

$$G^>(\mathbf{r} - \mathbf{r}') = \langle \theta_{>}(\mathbf{r}) \theta_{>}(\mathbf{r}') \rangle_0^> = \frac{k_B T}{\tilde{K}} \int_{\mathbf{q}}^> \frac{e^{i\mathbf{q} \cdot (\mathbf{r} - \mathbf{r}')}}{q^{2+\sigma}}, \quad (\text{A12})$$

with, for small $\ln b$, $G^>(\mathbf{0}) \approx S_d(\ln b) k_B T / [(2\pi)^d \tilde{K} \Lambda^\omega]$, with S_d the surface hyper-area of a d -dimensional unit ball.

The crucial $\frac{1}{2} \kappa (\nabla \theta)^2$ contribution arises from the second order term $-\frac{\beta}{2} \langle H_g^2 \rangle_{0>}^c$ in (A7). This term is

$$\langle H_g^2 \rangle_{0>}^c = g^2 \int_{\mathbf{r}, \mathbf{r}'} \left(\langle \cos[\theta_{<}(\mathbf{r}) + \theta_{>}(\mathbf{r})] \cos[\theta_{<}(\mathbf{r}') + \theta_{>}(\mathbf{r}')] \rangle - \langle \cos[\theta_{<}(\mathbf{r}) + \theta_{>}(\mathbf{r})] \rangle \langle \cos[\theta_{<}(\mathbf{r}') + \theta_{>}(\mathbf{r}')] \rangle \right). \quad (\text{A13})$$

Again writing the cosines in this expression in terms of

complex exponentials, performing the averages using the handy relation (A10), and gathering terms, we get

$$\begin{aligned} \langle H_g^2 \rangle_{0>}^c &= \frac{g^2}{2} \int_{\mathbf{r}, \mathbf{r}'} \left\{ \cos[\theta_{<}(\mathbf{r}) - \theta_{<}(\mathbf{r}')] \left(\exp\left[-\frac{1}{2} \langle (\theta_{>}(\mathbf{r}) - \theta_{>}(\mathbf{r}'))^2 \rangle\right] - \exp\left[-\langle \theta_{>}^2(\mathbf{r}) \rangle\right] \right) \right. \\ &\quad \left. + \cos[\theta_{<}(\mathbf{r}) + \theta_{<}(\mathbf{r}')] \left(\exp\left[-\frac{1}{2} \langle (\theta_{>}(\mathbf{r}) + \theta_{>}(\mathbf{r}'))^2 \rangle\right] - \exp\left[-\langle \theta_{>}^2(\mathbf{r}) \rangle\right] \right) \right\}. \end{aligned} \quad (\text{A14})$$

Now using the facts that

we can rewrite (A14) as

$$\begin{aligned} \langle H_g^2 \rangle_{0>}^c &\approx \frac{1}{2} g^2 e^{-G^>(\mathbf{0})} \int_{\mathbf{r}, \mathbf{r}'} \left[\mathcal{C}_+(|\mathbf{r} - \mathbf{r}'|) \cos[\theta_{<}(\mathbf{r}) - \theta_{<}(\mathbf{r}')] \right. \\ &\quad \left. + \mathcal{C}_-(|\mathbf{r} - \mathbf{r}'|) \cos[\theta_{<}(\mathbf{r}) + \theta_{<}(\mathbf{r}')] \right], \end{aligned} \quad (\text{A16})$$

$\langle (\theta_{>}(\mathbf{r}) \pm \theta_{>}(\mathbf{r}'))^2 \rangle = 2 \left\{ \langle (\theta_{>}^2(\mathbf{r})) \rangle \pm \langle \theta_{>}(\mathbf{r}) \theta_{>}(\mathbf{r}') \rangle \right\}$ where we have defined the kernels

$$= 2[G^>(\mathbf{0}) \pm G^>(\mathbf{r} - \mathbf{r}')], \quad (\text{A15}) \quad \mathcal{C}_{\pm}(\mathbf{r}) = e^{\pm G^>(\mathbf{r})} - 1. \quad (\text{A17})$$

Because these kernels $\mathcal{C}_\pm(\mathbf{r})$ only have support from high momenta (specifically, momenta near the UV cutoff $\Lambda \sim 1/a$), they are both short-ranged. Hence, we can Taylor-expand both cosines in (A16) in $\mathbf{r} - \mathbf{r}'$. For the second term, this simply generates, to leading order, a $\cos[2\theta(\mathbf{r})]$ term, which is a higher, less relevant harmonic that we will neglect. For the first term, this expansion gives $\delta H = \frac{1}{2}\kappa_R \int_{\mathbf{r}} (\nabla\theta)^2$, with $\kappa_R = \kappa + \delta\kappa$, where κ is the value of κ before we performed this step of the RG. For the very first step of the RG, $\kappa = 0$, but on subsequent steps, κ will be non-zero, precisely because of

its generation as outlined above. That calculation gives

$$\begin{aligned} \delta\kappa &\approx \frac{1}{8}g^2\beta e^{-G^>(0)} \int d^2r r^2 \mathcal{C}_+(r), \\ &\approx \frac{1}{16}g^2\beta \int d^2r r^2 G^2_>(r), \\ &\approx \frac{c_2 g^2 k_B T}{16\tilde{K}^2} \ln b, \end{aligned} \quad (\text{A18})$$

to leading order in $\ln b$. Here we have defined $c_2 \equiv (2 + \sigma)^2 / (2\pi\Lambda^{2(2+\sigma)})$. Note that c_2 remains constant under renormalization, since on each step of the RG we rescale lengths to restore the ultraviolet cutoff Λ to its original value.

In deriving this result (A18), we have neglected the contribution lowest order in $G^>(\mathbf{q})$, since it vanishes at $q = 0$. This is because, by definition, $G^>(\mathbf{q})$ only has support at high momenta near the UV cutoff Λ . We then evaluated the integral $I_2 \equiv \int d^2r r^2 G^2_>(r)$ as follows. First we expressed it as

$$I_2 \equiv \int d^2r r^2 G^2_>(r) = \int d^2r |\mathbf{r}G_>(r)|^2. \quad (\text{A19})$$

Then Fourier transforming, we can rewrite (A19) as

$$I_2 = \int_{\mathbf{q}}^> \text{FT}_{\mathbf{q}}[\mathbf{r}G_>(r)] \cdot \text{FT}_{-\mathbf{q}}[\mathbf{r}G_>(r)], \quad (\text{A20})$$

where $\text{FT}_{\mathbf{q}}[\mathbf{V}(\mathbf{r})]$ denotes the Fourier transform of any

position dependent vector $\mathbf{V}(\mathbf{r})$, evaluated at wavevector \mathbf{q} . We can thus express it in the convenient form,

$$\text{FT}_{\mathbf{q}}[\mathbf{r}G_>(r)] = \int d^2r \mathbf{r}G_>(\mathbf{r})e^{-i\mathbf{q}\cdot\mathbf{r}} = i\nabla_{\mathbf{q}} \int d^2r G_>(\mathbf{r})e^{-i\mathbf{q}\cdot\mathbf{r}} = i\nabla_{\mathbf{q}}G_>(\mathbf{q}), \quad (\text{A21})$$

where the vector operator $\nabla_{\mathbf{q}}$ denotes the gradient with respect to the vector \mathbf{q} . Given our earlier result (A12)

for $G_>(\mathbf{q})$, one can see that

$$i\nabla_{\mathbf{q}}G_>(\mathbf{q}) = -\frac{i(2+\sigma)\mathbf{q}}{q^{4+\sigma}} \left(\frac{k_B T}{\tilde{K}}\right). \quad (\text{A22})$$

Inserting this result, and the analogous expression for $\text{FT}_{-\mathbf{q}}[\mathbf{r}G_>(r)]$, into (A20) gives

$$I_2 = (2+\sigma)^2 \left(\frac{k_B T}{\tilde{K}}\right)^2 \int_{\mathbf{q}}^> \left(\frac{1}{q^{6+2\sigma}}\right) = \frac{(2+\sigma)^2}{2\pi\Lambda^{2(2+\sigma)}} \left(\frac{k_B T}{\tilde{K}}\right)^2 \ln b. \quad (\text{A23})$$

in $d = 2$, or, in general d ,

$$I_d = \frac{(2+\sigma)^2 S_d}{(2\pi)^d \Lambda^{2(3+\sigma)-d}} \left(\frac{k_B T}{\tilde{K}}\right)^2 \ln b \equiv c_d \left(\frac{k_B T}{\tilde{K}}\right)^2 \ln b. \quad (\text{A24})$$

Combining the above d -dimensional coarse-graining

analysis with the length rescaling (A6) gives the full re-

cursion relations for the renormalized couplings \tilde{K}_R , g_R , and κ_R in terms of the original couplings \tilde{K} , g , and κ (and, of course, the rescaling factor b):

$$\tilde{K}_R = \tilde{K}b^{-\omega}, \quad g_R = b^d g \exp\left(-\left[\frac{h_d k_B T}{2\tilde{K}}\right] \ln b\right), \quad \kappa_R = b^{d-2}\left(\kappa + \frac{c_d g^2 k_B T}{16\tilde{K}^2} \ln b\right), \quad (\text{A25})$$

where we have defined

$$h_d \equiv \frac{S_d \Lambda^{-\omega}}{(2\pi)^d}. \quad (\text{A26})$$

As is standard practice in RG calculations, we will now rewrite these recursion relations in differential form. To do this, we will choose the rescaling factor b to be very close to one. Specifically, we will take $b = 1 + d\ell$, with $d\ell$ differential. We also imagine iterating the renormalization group for n steps, and define a renormalization group “time” via $\ell \equiv nd\ell$. We now take the limit $d\ell \rightarrow 0$ and $n \rightarrow \infty$ such that the product $nd\ell = \ell$ remains finite.

Doing all of this, using the fact that, in the $d\ell \rightarrow 0$ limit, $\ln b \rightarrow d\ell$, considering the $n + 1$ ’st RG step, which takes us from $\ell = nd\ell$ to $\ell + d\ell$, and, finally, expanding in $d\ell$, we can rewrite (A25) as

$$\tilde{K}(\ell + d\ell) = \tilde{K}(\ell)(1 - \omega d\ell) + O(d\ell^2), \quad (\text{A27})$$

$$g(\ell + d\ell) = g(\ell) \left(1 + \left[d - h_d k_B T / [2\tilde{K}]\right] d\ell\right) + O(d\ell^2), \quad (\text{A28})$$

$$\kappa(\ell + d\ell) = \kappa(\ell) \left(1 + \left[(d-2) + \frac{c_d g^2 k_B T}{16\kappa\tilde{K}^2}\right] d\ell\right). \quad (\text{A29})$$

Now subtracting $\tilde{K}(\ell)$, $g(\ell)$, and $\kappa(\ell)$ from both sides of (A27), (A28), and (A29), respectively, dividing the resultant equations by $d\ell$, and taking the limit $d\ell \rightarrow 0$,

we obtain the differential recursion relations:

$$\frac{d\tilde{K}}{d\ell} = -\omega\tilde{K}, \quad (\text{A30})$$

$$\frac{dg}{d\ell} = \left(d - \frac{h_d k_B T}{2\tilde{K}}\right) g, \quad (\text{A31})$$

$$\frac{d\kappa}{d\ell} = (d-2)\kappa + \frac{c_d k_B T g^2}{16\tilde{K}^2}. \quad (\text{A32})$$

It is useful to define a dimensionless measure of temperature (or, equivalently, of the inverse of the stiffness \tilde{K}),

$$t(\ell) \equiv \frac{h_d k_B T}{2\tilde{K}(\ell)}, \quad (\text{A33})$$

in terms of which the flow equations reduce to

$$\frac{dt}{d\ell} = \omega t, \quad (\text{A34})$$

$$\frac{dg}{d\ell} = (d-t)g, \quad (\text{A35})$$

$$\frac{d\kappa}{d\ell} = (d-2)\kappa + \frac{f_d}{k_B T} t^2 g^2, \quad (\text{A36})$$

where we have defined

$$f_d \equiv \frac{(2+\sigma)^2 (2\pi)^d}{4S_d \Lambda^{d+2}}. \quad (\text{A37})$$

These recursion relations are straightforwardly solved, giving

$$t(\ell) = t_0 e^{\omega\ell}, \quad (\text{A38})$$

$$g(\ell) = g_0 e^{\ell d} \exp\left[-\frac{t_0}{\omega} (e^{\omega\ell} - 1)\right], \quad (\text{A39})$$

and

$$\kappa(\ell) = \frac{f_d t_0^2 g_0^2}{k_B T} e^{(d-2)\ell} \int_0^\ell d\ell' e^{(2\omega+d+2)\ell'} \exp\left[-\frac{2t_0}{\omega} (e^{\omega\ell'} - 1)\right], \quad (\text{A40})$$

where we have neglected the subdominant transient in $\kappa(\ell)$. Here t_0 and g_0 are the bare values of t and g . For $t_0 \ll 1$ and for $\ell \gg \frac{1}{\omega} \ln\left(\frac{\omega}{t_0}\right)$ the integral in this

expression has already converged, allowing us to extend

the upper limit of integration to $\ell \rightarrow \infty$. This gives

$$\kappa(\ell) \approx \frac{fdt_0^2g_0^2}{k_B T} e^{(d-2)\ell} \int_0^\infty d\ell' e^{(2\omega+d+2)\ell'} \exp\left[-\frac{2t_0}{\omega} e^{\omega\ell'}\right], \quad (\text{A41})$$

$$\begin{aligned} &\approx \frac{fdt_0g_0^2}{2k_B T} e^{(d-2)\ell} \left(\frac{\omega}{2t_0}\right)^{1+(d+2)/\omega} \Gamma(2+(d+2)/\omega), \\ &\equiv \alpha_d \frac{t_0^{-(d+2)/\omega} g_0^2}{k_B T \Lambda^{d+2}} e^{(d-2)\ell}, \end{aligned} \quad (\text{A42})$$

where $\alpha_d = (2+\sigma)^2 \left(\frac{\omega}{2}\right)^{\frac{d+2}{\omega}+1} (2\pi)^d \Gamma\left(\frac{d+2}{\omega}+2\right) / (4S_d)$ is a dimensionless, $O(1)$ constant.

Our solution (A38) for $t(\ell)$, combined with our expression (A33) relating $t(\ell)$ to $\tilde{K}(\ell)$, determines $\tilde{K}(\ell)$:

$$\tilde{K}(\ell) = \tilde{K}_0 e^{-\omega\ell}, \quad (\text{A43})$$

where $\tilde{K}_0 = \frac{(k_B T)^2}{K C(\sigma)} = \frac{(k_B T)^2 a^\omega}{K} \times O(1)$ is the "bare" (i.e., $\ell = 0$) value of \tilde{K} .

As mentioned above, we have ignored the effect of the generated $|\nabla\theta|^2$ coupling κ on the averages over $\theta_{>}$ that we perform in each step of the RG. This approximation will clearly break down at the RG time ℓ once the $\kappa(\ell)q^2|\theta(\mathbf{q})|^2$ part of the energy starts to become comparable to the $\tilde{K}(\ell)q^{2+\sigma}|\theta(\mathbf{q})|^2$ piece that we have kept for the \mathbf{q} 's of the $\theta(\mathbf{q})$'s over which we are averaging on each RG step. Since those \mathbf{q} 's are those near the Brillouin zone boundary $|\mathbf{q}| = \Lambda$, this leads to the condition

$$\kappa(\ell^*)\Lambda^2 = \tilde{K}(\ell^*)\Lambda^{2+\sigma}, \quad (\text{A44})$$

where we have defined ℓ^* as the value of ℓ at which the κ term starts to become important, and we recall that Λ is kept fixed under the RG transformation.

Using our solutions (A43) and (A42) for $\tilde{K}(\ell)$ and $\kappa(\ell)$ in this condition (A44) enables us to solve for e^{ℓ^*} :

$$e^{\ell^*} = \left(\frac{k_B T \tilde{K}_0 t_0^{\frac{d+2}{\omega}} \Lambda^{d+2+\sigma}}{\alpha_d g_0^2}\right)^{1/\sigma}, \quad (\text{A45})$$

$$\approx \left[\left(\frac{K}{k_B T}\right)^{\frac{d+2}{\omega}-1} \left(\frac{1}{y^2}\right)\right]^{1/\sigma} \times O(1). \quad (\text{A46})$$

In writing the second equality, we have used equations (14) and (17) of the main text, evaluated in the "bare" ($\ell = 0$) system, to relate \tilde{K}_0 and $g_0 \equiv g_1(\ell = 0)$, respectively to the original parameters of the super-Coulombic gas model. We have also used equation (A33) evaluated at $\ell = 0$ for t_0 . Finally, in the last step, we have taken the ultraviolet cutoff $\Lambda \sim 1/a$.

As usual in the RG, we can associate with this renormalization group time ℓ^* a crossover length scale

$$\begin{aligned} \xi &= a e^{\ell^*} \\ &= a \left[\left(\frac{K}{k_B T}\right)^{\frac{d+2}{\omega}-1} \left(\frac{1}{y^2}\right)\right]^{1/\sigma} \times O(1), \end{aligned} \quad (\text{A47})$$

which is the result quoted in the main text.

A standard RG analysis implies that the physical value κ_{phys} of κ – that is, the value that will be observed in experiment – can be obtained from the renormalized value $\kappa(\ell^*)$ by undoing the effect of all the rescalings we did in the RG. This can be seen to imply

$$\begin{aligned} \kappa_{\text{phys}} &= e^{(2-d)\ell^*} \kappa(\ell^*) \\ &= \frac{t_0^{-\frac{d+2}{\omega}} g_0^2}{k_B T \Lambda^{d+2}} = k_B T \left(\frac{k_B T}{K}\right)^{\frac{d+2}{\omega}} y^2 a^{2-d} \times O(1), \\ &= k_B T \left(\frac{k_B T}{K}\right)^{\frac{d+2}{\omega}} a^{2-d} e^{-2E_c/k_B T} \times O(1), \\ &= \frac{(k_B T)^2}{K} \left(\frac{a}{\xi}\right)^\sigma a^{2-d} \times O(1). \end{aligned} \quad (\text{A48})$$

In the main text we drop the subscript "phys" on κ_{phys} and refer to this stiffness simply as κ .

The most important point about this result is that the renormalized value κ_{phys} of the parameter κ is not zero, even though it *is* zero in the original bare model. By simply reversing the steps of the duality manipulations that lead from our original super-Coulombic gas model to the sine-Gordon theory, it is easy to see that the existence of a non-zero κ_{phys} implies that the effective renormalized interaction between test charges becomes Coulombic if the test charges are separated by a distance greater than the crossover length ξ . This is our most important conclusion: a longer-ranged than Coulombic interaction between charges *always* "screens down" to a purely Coulombic interaction at sufficiently long distances, in all spatial dimensions.

Quantitatively, the effective interaction on those longer length scales, beyond ξ , is given by:

$$H = \frac{1}{2} \sum_{\mathbf{r}, \mathbf{r}'} n_{\mathbf{r}} U_{\text{eff}}(\mathbf{r} - \mathbf{r}') n_{\mathbf{r}'} + E_c \sum_{\mathbf{r}} n_{\mathbf{r}}^2, \quad (\text{A49})$$

with $U_{\text{eff}}(\mathbf{r})$ given by

$$U_{\text{eff}}(\mathbf{r}) = U_{\text{Coulomb}}(\mathbf{r}) = \begin{cases} \frac{(k_B T)^2}{S_d \kappa} r^{2-d}, & d > 2, \\ -\frac{(k_B T)^2}{2\pi\kappa} \ln\left(\frac{r}{a}\right), & d = 2. \end{cases} \quad (\text{A50})$$

Concomitant with this screening, we predict that the 2D super-Coulombic plasma undergoes a KT transition at a temperature T_{KT} that satisfies[11]

$$\frac{k_B T_{KT}}{2\pi\kappa(T_{KT})} = 4. \quad (\text{A51})$$

Using our expression (A48) for $\kappa(T)$, evaluated in $d = 2$, in this condition (A51) gives

$$\left(\frac{K}{k_B T_{KT}}\right)^{4/\sigma} e^{2E_c/k_B T} = O(1). \quad (\text{A52})$$

whose solution is

$$k_B T_{KT} = \frac{\sigma E_c}{2W_0\left(\frac{\sigma E_c}{2Ka\sigma}\right)} \quad (\text{A53})$$

where $W_0(x)$ is the $k = 0$ branch of the Lambert W function.

Appendix B: Dielectric screening analysis

Here we present the details of the calculation of the electric susceptibility, χ used in the main text to compute the screening length ξ . To this end we simply need to calculate the mean dipole moment $\langle \mathbf{p} \rangle$ density in the presence of a local "electric field" $\mathbf{E} = -\nabla U(\mathbf{r})$, which we take to be uniform over the distance of the separation of the pair. (It is straightforward to show that higher charges make a far smaller contribution to the susceptibility at low temperatures, and so may be ignored.)

The mean dipole moment $\langle \mathbf{p} \rangle$ density can be calculated for an isolated $n_\alpha = \pm 1$ pair of unit charges using simple Boltzmann statistics. This calculation is straightforward if we are in a range of parameters such that two conditions are met: 1) The mean size (i.e., distance between its constituent ± 1 charges) of an isolated dipole pair is large compared to the lattice constant a , so that we can treat the dipole in the continuum approximation. This requires that

$$\left(\frac{K}{k_B T}\right) a^\omega \ll 1. \quad (\text{B1})$$

2) The local density of dipoles must be small enough that each dipole pair can be treated in isolation. This requires that the charge fugacity

$$y \equiv e^{\frac{-E_c}{k_B T}} \ll 1. \quad (\text{B2})$$

Both conditions (B1) and (B2) can be satisfied in the temperature range

$$E_c \gg k_B T \gg K a^\omega. \quad (\text{B3})$$

as long as $E_c \gg K a^\omega$.

One physical example of such a situation would be a system in which the total number of positive and negative charges are separately conserved, and the density of each is small. In such a system, one would treat the core energy E_c as a type of a "Lagrange multiplier", whose value would have to be chosen to keep the densities of the charges small. This would mean that E_c would become proportional to $k_B T$, so as to keep the charge density fixed as temperature is varied. The fixed ratio of E_c to $k_B T$ would also have to be large if the density of charges was small. Thus we would have the first part of the condition (B3) (i.e., $E_c \gg k_B T$) automatically satisfied at all temperatures. The second condition (i.e.,

$k_B T \gg K a^\omega$) could then be always satisfied by raising temperature sufficiently.

In general spatial dimension d the i 'th component of the mean dipole moment $\langle \mathbf{p} \rangle$ density can be obtained as follows. First, let us put our system on a hypercubic lattice of lattice constant a . Now, considering a hypercubic sub-volume $V_s = L_s^d$ of the system whose lateral extent $L_s \gg a$, but assume L_s is still small enough that, in a typical configuration there are no dipoles in the volume at all. Since the maximum possible dipole density is y^2/a^d , which applies when the two elements of the dipole are separated by one lattice constant, we can therefore achieve this by requiring that

$$a^d \ll V_s \ll a^d/y^2. \quad (\text{B4})$$

We can now think of this sub-volume as being a system in the Grand Canonical Ensemble, with the remainder of the system acting as the heat and particle bath. Hence, the probability $P(\mathbf{r})$ of having a single pair of oppositely charged ± 1 dipoles with separation \mathbf{r} in the sub-volume is

$$P(\mathbf{r}) = \left(\frac{V_s}{a^d}\right) \exp(-(-U_0(\mathbf{r}) + 2E_c)/k_B T)/\mathcal{Q}, \quad (\text{B5})$$

where \mathcal{Q} is the Grand Canonical Partition function for the sub-volume V_s , and the factor $\left(\frac{V_s}{a^d}\right)$ is simply the number of sites in the volume on which the first charge of the pair can be placed. (Once that first charge is positioned, the second charge can only be a displacement *vector* \mathbf{r} away, so there is no further choice as to where to put that charge.)

The Grand Canonical partition function is, as always, a sum of the Boltzmann weight over configurations with different numbers of charges in the volume V_s , starting with the configuration with *no* charges, for which the Boltzmann weight is 1 (since the energy of a charge free state is zero). Hence we have

$$\mathcal{Q} = 1 + O\left[y^2 \left(\frac{V_s}{a^d}\right)\right] \approx 1, \quad (\text{B6})$$

where the second approximate equality follows from the fact that, by construction $y^2 \left(\frac{V_s}{a^d}\right) \ll 1$, by the second strong inequality of (B4).

Using (B6) in (B5) gives

$$P(\mathbf{r}) \approx \left(\frac{V_s}{a^d}\right) e^{-[-U_0(\mathbf{r})+2E_c]/k_B T}. \quad (\text{B7})$$

It is also clear that the second strong inequality of (B4) implies that it is extremely unlikely that there will be *more* than one dipole in volume V_s , or that there are dipoles made of higher than unit charges. It also implies that higher moment configurations, such as, e.g., quadrupoles, which can be thought of as configurations with more than one dipole pair close to each other, are also highly unlikely, and therefore also negligible. Hence,

the only configuration that makes an appreciable contribution to the total dipole moment \mathcal{P} is the single dipole configuration whose probability we just calculated. (The zero dipole state obviously contributes nothing to the dipole moment.)

Since the dipole moment of a single pair is just the vector \mathbf{r} separating the two charges, we have

$$\begin{aligned} \langle \mathcal{P} \rangle &= \sum_{\mathbf{r}} \mathbf{r} P(\mathbf{r}) \\ &\approx y^2 \left(\frac{V_s}{a^d} \right) \sum_{\mathbf{r}} \exp \left(\frac{-(K(r/a)^\omega - \mathbf{E} \cdot \mathbf{r})}{k_B T} \right) \mathbf{r}, \end{aligned} \quad (\text{B8})$$

where we have added an external "electric field" energy $\sum_{\mathbf{r}} \mathbf{E} \cdot \mathbf{r}$. Our goal is to calculate the susceptibility to this applied field.

Dividing both sides of (B8) by the volume V_s of our sub-region gives the mean dipole moment per unit volume $\langle \mathbf{p} \rangle$:

$$\begin{aligned} \langle \mathbf{p} \rangle &= V_s^{-1} \sum_{\mathbf{r}} \mathbf{r} P(\mathbf{r}) \\ &\approx \left(\frac{y^2}{a^{2d}} \right) \int d^d r \exp \left(\frac{-(K(r/a)^\omega - \mathbf{E} \cdot \mathbf{r})}{k_B T} \right) \mathbf{r}, \end{aligned} \quad (\text{B9})$$

where in the second equality we have used our expression (B7) for $P(\mathbf{r})$, and gone over to the continuum limit in the usual way, i.e., via the replacement of sums over \mathbf{r} with integrals over \mathbf{r} using the substitution $\sum_{\mathbf{r}} \rightarrow a^{-d} \int d^d r$

The i 'th component of this vectorial equation therefore reads

$$\begin{aligned} \langle p_i \rangle &= \langle r_i \rangle = \left(\frac{y^2}{a^{2d}} \right) \int \exp \left(\frac{-(K(r/a)^\omega - \mathbf{E} \cdot \mathbf{r})}{k_B T} \right) r_i d^d r \\ &\approx \left(\frac{y^2}{a^{2d} k_B T} \right) \int \exp \left(-\frac{K(r/a)^\omega}{k_B T} \right) r_i r_j E_j d^d r, \end{aligned} \quad (\text{B10})$$

where in the second equality we have expanded to linear order in \mathbf{E} .

Taking advantage of the rotational symmetry of the Boltzmann factor $\exp \left(-\frac{K(r/a)^\omega}{k_B T} \right)$, we can replace $r_i r_j$ in the integral by its angular average $\frac{r_i^2}{d} \delta_{ij}$, which reduces (B10) to

$$\langle p_i \rangle = \left[\frac{y^2}{d a^{2d} k_B T} \int \exp \left(-\frac{K(r/a)^\omega}{k_B T} \right) r^2 d^d r \right] E_i. \quad (\text{B11})$$

That is, we find $\langle \mathbf{p} \rangle = \chi \mathbf{E}$, with the susceptibility χ given

by

$$\begin{aligned} \chi &= \frac{y^2}{d a^{2d} k_B T} \int \exp \left(-\frac{K(r/a)^\omega}{k_B T} \right) r^2 d^d r \\ &= \frac{S_d \Gamma \left(\frac{d+2}{\omega} \right) y^2}{\omega d k_B T a^{d-2}} \left(\frac{k_B T}{K} \right)^{\left(\frac{d+2}{\omega} \right)} \\ &= \frac{y^2}{k_B T a^{d-2}} \left(\frac{k_B T}{K} \right)^{\left(\frac{d+2}{\omega} \right)} \times O(1). \end{aligned} \quad (\text{B12})$$

Using this result in our expression (33) for the crossover length ξ between super-Coulombic and Coulombic interactions gives

$$\xi = a^{\frac{d}{\sigma}} (K\chi)^{-\frac{1}{\sigma}} = a \left[\left(\frac{K}{k_B T} \right)^{\left(\frac{d+2}{\omega} \right) - 1} \left(\frac{1}{y^2} \right) \right]^{\frac{1}{\sigma}} \times O(1) \quad (\text{B13})$$

in perfect agreement with the result (A47) obtained earlier by the renormalization group analysis of the sine-Gordon theory.

Appendix C: Computational details of Fourier transforms

In this appendix we demonstrate:

1) Equation (4) of the main text, by showing that the Fourier transform of

$$U_0(q) = C(\sigma, d) K / q^{2+\sigma} \quad (\text{C1})$$

back to real space does indeed give the bare interaction potential given by (2) of the main text,

$$U_0(r) = -K(r/a)^\omega, \quad \omega = 2 - d + \sigma, \quad (\text{C2})$$

and

2) that the asymptotic long-distance tail of the real-space Debye-Huckel screened effective potential is power-law $U_{\text{eff}}(r) = C_{DH}(\sigma, d) / r^{d+2+\sigma}$. In the process, we also calculate the constants $C_{DH}(\sigma, d)$ and $C(\sigma, d)$. Our result for the former implies overscreening for all super-Coulombic potentials, as discussed in the main text.

1. Fourier transform of the bare potential when it is (naively) binding (i.e., $\omega > 0$)

Point 1) is slightly subtle to derive, because, in fact, the Fourier transform of (C1) back to real space contains, in addition to the bare potential $U_0(r)$ given by equation (C2), an additive constant which diverges for all binding potentials (that is, all potentials with $\omega > 0$) like L^ω , where L is the linear spatial extent of the system in real space. Fortunately, this additive constant, which also depends on the macroscopic shape of the system, has

no effect on the physics of the problem, other than (in the grand-canonical ensemble) to enforce the constraint of overall charge neutrality, which we expect to hold on physical grounds for confining potentials. Once charge neutrality is enforced, this additive constant drops out of the problem, as we will show below.

Since we need to consider a finite system in order to get a finite answer, we begin by formulating Fourier transforms in a finite system. We will take our system to be a d -dimensional rectilinear slab with $d - 1$ of its edge lengths given by L_\perp , and a single edge length L_z , which need not equal L_\perp in general. (This will enable us to investigate the aspect ratio dependence of the aforementioned additive constant.)

For computational convenience, we will use periodic boundary conditions on this rectangular box, and define the Fourier transformed charge density $n(\mathbf{q})$ via

$$n(\mathbf{q}) = \frac{1}{\sqrt{V}} \int d^d r e^{-i\mathbf{q}\cdot\mathbf{r}} n(\mathbf{r}), \quad (\text{C3})$$

where

$$V = L_\perp^{d-1} L_z \quad (\text{C4})$$

is the (hyper) volume of the system, and the values of \mathbf{q} allowed by our periodic boundary conditions are

$$\mathbf{q} = \frac{2\pi n_z}{L_z} \hat{\mathbf{z}} + \frac{2\pi}{L_\perp} \hat{\mathbf{n}}_\perp, \quad (\text{C5})$$

where all of the components of

$$\hat{\mathbf{n}} = n_z \hat{\mathbf{z}} + \hat{\mathbf{n}}_\perp \quad (\text{C6})$$

are integers. We exclude $\mathbf{0}$ from the allowed values of \mathbf{n} to exclude $\mathbf{q} = \mathbf{0}$ from the sum over \mathbf{q} .

We now take the Hamiltonian to be

$$H = \frac{1}{2} \sum_{\mathbf{q}} \frac{C(\sigma, d)K}{q^{2+\sigma}} |n(\mathbf{q})|^2 + E_c \sum_{\mathbf{r}} n_{\mathbf{r}}^2, \quad (\text{C7})$$

and see if we can make a choice of $C(\sigma, d)$ that recovers our potential (2), (C2), plus an additive constant. Inserting (C3) into (C7), we find that to recover (2), we must have

$$U_0(\mathbf{r}) = \frac{C(\sigma, d)K}{V} \sum_{\mathbf{q}} \frac{e^{i\mathbf{q}\cdot\mathbf{r}}}{q^{2+\sigma}}. \quad (\text{C8})$$

We now rewrite the sum in this expression as

$$S(\mathbf{r}) = \frac{1}{V} \sum_{\mathbf{q}} \frac{e^{i\mathbf{q}\cdot\mathbf{r}}}{q^{2+\sigma}}, \quad (\text{C9})$$

$$= \frac{1}{V} \sum_{\mathbf{q}} \frac{1}{q^{2+\sigma}} + \frac{1}{V} \sum_{\mathbf{q}} \frac{(e^{i\mathbf{q}\cdot\mathbf{r}} - 1)}{q^{2+\sigma}}. \quad (\text{C10})$$

The first term in this expression (which we call S_0) is given by

$$S_0 = \frac{1}{V} \sum_{\mathbf{q}} \frac{1}{q^{2+\sigma}}, \quad (\text{C11})$$

$$= \frac{1}{L_\perp^{d-1} L_z} \sum_{\hat{\mathbf{n}} \neq \mathbf{0}} \left[\frac{1}{n_z^2 (2\pi/L_z)^2 + n_\perp^2 (2\pi/L_\perp)^2} \right]^{1+\sigma/2}, \quad (\text{C12})$$

$$= \frac{L_\perp^\omega f^{1+\sigma}}{(2\pi)^{2+\sigma}} g(f). \quad (\text{C13})$$

where we have defined aspect ratio

$$f = \frac{L_z}{L_\perp} \quad (\text{C14})$$

and

$$g(f) = \sum_{\hat{\mathbf{n}} \neq \mathbf{0}} \left[\frac{1}{n_z^2 + f^2 n_\perp^2} \right]^{1+\sigma/2}. \quad (\text{C15})$$

Note that the sum in (C15) converges as $\mathbf{n} \rightarrow \infty$ if and only if (iff) $\omega > 0$, which is the case we are considering here.

Note also that the dependence of S_0 on f demonstrates the shape dependence of this additive constant. Such shape dependence also occurs due to dipolar interactions in ferromagnets, as here, this is due to the long-ranged nature of the interaction.

The two most important points to note about S_0 are: (i) it is constant, and (ii) it diverges as system size $L_\perp \rightarrow \infty$ (keeping f fixed). Point (ii) might appear quite alarming. Fortunately, point (i) renders the S_0 term almost completely unimportant. Indeed, one can easily see that it leads to a term in the total Hamiltonian

$$H_{S_0} = \frac{1}{2} S_0 \int_{\mathbf{r}, \mathbf{r}'} n(\mathbf{r}) n(\mathbf{r}'), \quad (\text{C16})$$

$$= \frac{1}{2} S_0 \left(\int_{\mathbf{r}} n(\mathbf{r}) \right)^2 = Q^2 S_0, \quad (\text{C17})$$

where

$$Q \equiv \int_{\mathbf{r}} n(\mathbf{r}) \quad (\text{C18})$$

is the total charge in the system. Because the charges are quantized, any non-zero Q^2 must have a magnitude of at least 1. Hence, any non-neutral configuration of charges has a positive definite energy cost that diverges as L_\perp^ω , and, therefore, has a zero Boltzmann weight. That is, the effect of this S_0 term is to enforce total charge neutrality, which is a physical constraint we expect in a system with interactions that diverge at large \mathbf{r} .

Once the constraint of charge neutrality, $Q = 0$, is enforced, the S_0 term drops out of the Hamiltonian entirely. Hence, we are left with the model (1), with $U_0(\mathbf{r})$ given by the second term in (C10).

The sum in this term converges as the system size $L_{\perp,z} \rightarrow \infty$ (at fixed $f = L_z/L_{\perp}$), as we will show in a moment. This enables us to replace the sum on \mathbf{q} with an integral over \mathbf{q} by the usual replacement

$$\frac{1}{V} \sum_{\mathbf{q}} \dots \rightarrow \int \frac{d^d q}{(2\pi)^d} \dots \quad (\text{C19})$$

Doing this gives

$$U_0(\mathbf{r}) = C(\sigma, d)K \int \frac{d^d q}{(2\pi)^d} \frac{e^{i\mathbf{q}\cdot\mathbf{r}} - 1}{q^{2+\sigma}}. \quad (\text{C20})$$

Choosing a (hyper)-spherical coordinate system for \mathbf{q} with its polar axis aligned along \mathbf{r} , and evaluating the integral over the $d-2$ angular co-ordinates other than the polar angle θ gives

$$U_0(\mathbf{r}) = C(\sigma, d)K \frac{S_{d-1}}{(2\pi)^d} \int_0^\pi (\sin \theta)^{d-2} d\theta \times \int_\epsilon^\infty \frac{(e^{iqr \cos \theta} - 1)}{q^{1+\omega}} dq, \quad (\text{C21})$$

where S_{d-1} is the surface area of a $d-1$ -dimensional unit ball, and $\epsilon = O(L^{-1})$ (for simplicity focussing on aspect ratio $f = 1$) is an infra-red cutoff, crudely reflecting the discrete nature of the \mathbf{q} 's in our finite system. We will eventually consider the thermodynamic limit $L \rightarrow \infty$, corresponding to $\epsilon \rightarrow 0$, and will show that this limit is well-defined and finite for all $\omega < 2$.

Integrating over q in (C21) by parts gives

$$\int_\epsilon^\infty \frac{(e^{iqr \cos \theta} - 1)}{q^{1+\omega}} dq = -\omega^{-1} q^{-\omega} (e^{iqr \cos \theta} - 1) \Big|_\epsilon^\infty + i\omega^{-1} r \cos \theta \int_\epsilon^\infty \frac{e^{iqr \cos \theta}}{q^\omega} dq. \quad (\text{C22})$$

The first term in this expression vanishes at infinity, while its lower limit, for small ϵ (that is, large system size L) can be evaluated by Taylor-expanding the complex exponential, giving

$$q^{-\omega} (e^{iqr \cos \theta} - 1) \Big|_\epsilon^\infty = -i\epsilon^{1-\omega} r \cos \theta + \frac{1}{2}\epsilon^{2-\omega} r^2 \cos^2 \theta. \quad (\text{C23})$$

The first term in this expression vanishes when integrated over the polar angle θ . The second term vanishes in the thermodynamic limit $\epsilon \rightarrow 0$ for all $\omega < 2$. Hence, for all $\omega < 2$, in the limit $\epsilon \rightarrow 0$, the first, boundary term in (C22) can be dropped, leaving

$$U_0(\mathbf{r}) = iC(\sigma, d)K \frac{S_{d-1}}{\omega(2\pi)^d} r \int_0^\pi \sin^{d-2} \theta \cos \theta d\theta \times \int_\epsilon^\infty \frac{e^{iqr \cos \theta}}{q^\omega} dq. \quad (\text{C24})$$

This is as far as we can go for general ω in the range $0 < \omega < 2$. To go further, we must separately deal with the cases $0 < \omega < 1$ and $1 < \omega < 2$.

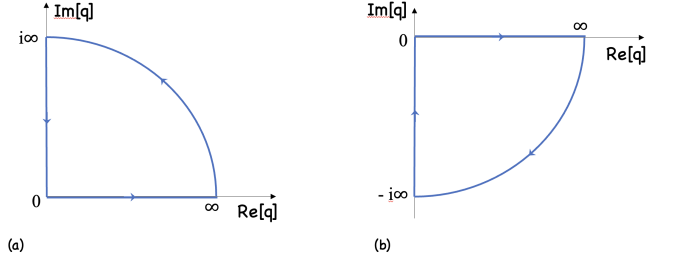


FIG. 3. Integration contours in the complex q space for $\cos \theta > 0$ in (a) and for $\cos \theta < 0$ in (b).

a. $0 < \omega < 1$

For $\omega < 1$, the integral over q in (C24) obviously converges as $q \rightarrow 0$. Hence, we can take the limit $\epsilon \rightarrow 0$. This leaves us with the task of evaluating

$$I(r \cos \theta) = \int_0^\infty \frac{e^{iqr \cos \theta}}{q^\omega} dq. \quad (\text{C25})$$

This can be done by rotating the contour in the complex plane, as illustrated by Fig.3. This rotation can be done since the closed contour does not enclose any poles and $q^{-\omega}$ vanishes as $q \rightarrow \infty$, making the integral over the quarter circle in these contour integrals vanish. The vanishing of $q^{-\omega}$ as $q \rightarrow \infty$ also ensures the convergence of the integral along the real axis, since an extra power of convergence is gained from strongly oscillatory factor.

For $\cos \theta > 0$, (i.e., for $0 < \theta < \pi/2$), we close the contour in the upper right quadrant 3(a) and obtain

$$I(r \cos \theta) = \int_0^\infty \frac{e^{iqr \cos \theta}}{q^\omega} dq. \quad (\text{C26})$$

Changing variable of integration from q to t , defined by $t \equiv qr \cos \theta$, we obtain

$$I(r \cos \theta) = ie^{-i\omega\pi/2} (\cos \theta)^{\omega-1} \Gamma(1-\omega) r^{\omega-1}. \quad (\text{C27})$$

The calculation for $\cos \theta < 0$, (i.e., for $\pi/2 < \theta < \pi$) is almost identical, except that we now close the contour in the lower right quadrant, 3(b) and obtain

$$I(r \cos \theta) = -ie^{i\omega\pi/2} (-\cos \theta)^{\omega-1} \Gamma(1-\omega) r^{\omega-1}. \quad (\text{C28})$$

Using these results (C27) and (C28) in (C24), we obtain

$$U_0(\mathbf{r}) = -Kr^\omega \frac{C(\sigma, d)S_{d-1}\Gamma(1-\omega)}{\omega(2\pi)^d} \times \left[-e^{-i\omega\pi/2} \int_0^{\pi/2} (\sin \theta)^{d-2} (\cos \theta)^\omega d\theta + e^{i\omega\pi/2} \int_{\pi/2}^\pi (\sin \theta)^{d-2} (-\cos \theta)^{\omega-1} \cos \theta d\theta \right] \quad (\text{C29})$$

With the change of variables $\phi = \pi - \theta$ in the second integral over θ , we see that it is equal to minus the first integral, which is tabulated[23]. We therefore choose $C(\sigma, d)$ such that

$$\begin{aligned} & \frac{C(\sigma, d) \cos(\omega\pi/2)\Gamma(1-\omega)\Gamma((\omega+1)/2)\Gamma((d-1)/2)S_{d-1}}{\omega(2\pi)^d\Gamma((2+\sigma)2)} \\ &= a^{-\omega}, \end{aligned} \quad (\text{C30})$$

and thereby obtain equations (2) and (4) of the Introduction, with

$$C(\sigma, d) = \frac{a^{-\omega}\omega(2\pi)^d\Gamma((2+\sigma)2)}{\cos(\omega\pi/2)\Gamma(1-\omega)\Gamma((\omega+1)/2)\Gamma((d-1)/2)S_{d-1}}. \quad (\text{C31})$$

Using

$$S_{d-1} = \frac{2\pi^{(\frac{d-1}{2})}}{\Gamma(\frac{d-1}{2})} \quad (\text{C32})$$

in (C31), we obtain

$$C(\sigma, d) = \frac{2^{d-1}\pi^{(d+1)/2}\omega\Gamma(2+\sigma)}{a^\omega \cos(\omega\pi/2)\Gamma(1-\omega)\Gamma((\omega+1)/2)}. \quad (\text{C33})$$

b. $1 < \omega < 2$

For $\omega > 1$, the integral in (C24) clearly does *not* converge as $\epsilon \rightarrow 0$. To overcome this problem, we first integrate by parts, obtaining

$$\begin{aligned} & \int_\epsilon^\infty \frac{e^{iqr \cos \theta}}{q^\omega} dq = \frac{1}{1-\omega} q^{1-\omega} e^{iqr \cos \theta} \Big|_\epsilon^\infty \\ & - \frac{i}{1-\omega} r \cos \theta \int_\epsilon^\infty e^{iqr \cos \theta} q^{1-\omega} dq. \end{aligned} \quad (\text{C34})$$

The first term inside the square brackets in this expression now vanishes at infinity, while at the lower limit, for very small ϵ , it becomes $\epsilon^{1-\omega}$. Since this is independent of θ , when multiplied by $\cos \theta$ and integrated over θ it vanishes as in (C24). Thus we are left with the second term, which now converges as $\epsilon \rightarrow 0$ for $\omega < 2$. We therefore take the limit $\epsilon \rightarrow 0$ in this remaining term and obtain

$$\begin{aligned} U_0(\mathbf{r}) &= C(\sigma, d)K \frac{S_{d-1}}{\omega(1-\omega)(2\pi)^d} r^2 \int_0^\pi \sin^{d-2} \theta \cos^2 \theta d\theta \\ &\times \int_0^\infty e^{iqr \cos \theta} q^{1-\omega} dq. \end{aligned} \quad (\text{C35})$$

The integral over q in this expression can now be evaluated by exactly the same sort of complex contour techniques that we used in the previous subsection, because the integrand vanishes for $q \rightarrow \infty$ since $\omega > 1$. We thereby obtain

$$\int_0^{i\infty} \frac{e^{iqr \cos \theta}}{q^{\omega-1}} dq = -e^{-i\omega\pi/2} (r \cos \theta)^{\omega-2} \Gamma(2-\omega), \quad (\text{C36})$$

for $\cos \theta > 0$, and

$$\int_0^{-i\infty} \frac{e^{iqr \cos \theta}}{q^{\omega-1}} dq = -e^{i\omega\pi/2} (-r \cos \theta)^{\omega-2} \Gamma(2-\omega), \quad (\text{C37})$$

for $\cos \theta < 0$. Using these results in (C35) gives

$$\begin{aligned} U_0(\mathbf{r}) &= Kr^\omega \frac{C(\sigma, d)S_{d-1}\Gamma(2-\omega)}{\omega(1-\omega)(2\pi)^d} \\ &\times \left[e^{-i\omega\pi/2} \int_0^{\pi/2} (\sin \theta)^{d-2} (\cos \theta)^\omega d\theta \right. \\ &\left. + e^{i\omega\pi/2} \int_{\pi/2}^\pi (\sin \theta)^{d-2} (-\cos \theta)^{\omega-2} \cos^2 \theta d\theta \right] \end{aligned} \quad (\text{C38})$$

With the change of variables $\phi = \pi - \theta$ in the second integral over θ , we see that it is equal to the first integral, which is tabulated[23]. We thereby obtain exactly our earlier result (C33) for $C(\sigma, d)$, after using the relation $\Gamma(2-\omega) = (1-\omega)\Gamma(1-\omega)$, thereby extending the validity of the result to $0 < \omega < 2$.

2. Non-binding potentials ($\omega < 0$)

For non-binding potentials ($\omega < 0$), it is possible to directly calculate the Fourier transform from real space to Fourier space:

$$\begin{aligned} U_0(\mathbf{q}) &= \int d^d r U_0(\mathbf{r}) e^{-i\mathbf{q}\cdot\mathbf{r}}, \\ &= -\frac{K}{a^\omega} \int d^d r r^\omega e^{-i\mathbf{q}\cdot\mathbf{r}}. \end{aligned} \quad (\text{C39})$$

Once again, different values of ω require different approaches to perform this integral.

a. $-2 < \omega < 0$

In this case, the integral is most conveniently done in Cartesian coordinates, with one axis, which we will call r_\parallel , running along $-\mathbf{q}$, and the other $d-1$ axes, which we will denote by \mathbf{r}_\perp running perpendicular to \mathbf{q} . With this choice of coordinates, the expression (C39) for $U_0(\mathbf{q})$ becomes

$$U_0(\mathbf{q}) = -\frac{K}{a^\omega} \int d^{d-1} r_\perp \int_{-\infty}^\infty dr_\parallel (r_\parallel^2 + r_\perp^2)^{\omega/2} e^{iqr_\parallel}. \quad (\text{C40})$$

The integrand in this expression considered as a function of complex r_\parallel has a branch cut along the positive imaginary axis, running from ir_\perp to $i\infty$. We close the contour in the complex plane around this branch cut, as illustrated in Fig. (4). Because the integrand vanishes

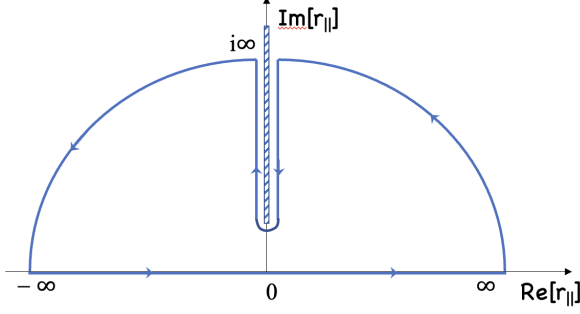


FIG. 4. Integration contour in the complex r_{\parallel} plane.

as $r_{\parallel} \rightarrow \infty$ for $\omega < 0$, we can close this contour in the complex plane with impunity. We thereby obtain

$$I(r_{\perp}) = \int_{-\infty}^{\infty} dr_{\parallel} (r_{\parallel}^2 + r_{\perp}^2)^{\omega/2} e^{iqr_{\parallel}}, \quad (\text{C41})$$

$$= \int_{ir_{\perp}}^{\infty} dr_{\parallel} (r_{\parallel}^2 + r_{\perp}^2)_{+}^{\omega/2} e^{iqr_{\parallel}} - \int_{ir_{\perp}}^{\infty} dr_{\parallel} (r_{\parallel}^2 + r_{\perp}^2)_{-}^{\omega/2} e^{iqr_{\parallel}} \quad (\text{C42})$$

where $(r_{\parallel}^2 + r_{\perp}^2)_{+}^{\omega/2}$ denotes the value of $(r_{\parallel}^2 + r_{\perp}^2)^{\omega/2}$ on the right hand side of the cut, and $(r_{\parallel}^2 + r_{\perp}^2)_{-}^{\omega/2}$ its value on the left hand side of the cut. Making the change of variable of integration $r_{\parallel} = it$ on both sides of the cut, with t real, we have

$$(r_{\parallel}^2 + r_{\perp}^2)_{\pm}^{\omega/2} = e^{\pm i\omega\pi/2} (t^2 - r_{\perp}^2)^{\omega/2}. \quad (\text{C43})$$

Thus we obtain

$$I(r_{\perp}) = -2 \sin(\omega\pi/2) \int_{r_{\perp}}^{\infty} dt (t^2 - r_{\perp}^2)^{\omega/2} e^{-qt}, \quad (\text{C44})$$

$$= -2r_{\perp}^{\omega+1} \sin(\omega\pi/2) \int_0^{\infty} d\phi (\sinh \phi)^{\omega+1} e^{-qr_{\perp} \cosh \phi}, \quad (\text{C45})$$

where in the second equality we changed variables of integration from t to ϕ via $t = r_{\perp} \cosh \phi$

Substituting this into our expression (C40) for $U_0(\mathbf{q})$ gives

$$U_0(\mathbf{q}) = 2Ka^{-\omega} \sin(\omega\pi/2) \int_0^{\infty} d\phi (\sinh \phi)^{\omega+1} \times \int d^{d-1} r_{\perp} r_{\perp}^{\omega+1} e^{-qr_{\perp} \cosh \phi}, \quad (\text{C46})$$

$$= \left(\frac{K}{a^{\omega} q^{2+\sigma}} \right) 2 \sin(\omega\pi/2) S_{d-1} \Gamma(2 + \sigma) \times \int_0^{\infty} d\phi \frac{(\sinh \phi)^{\omega+1}}{(\cosh \phi)^{2+\sigma}} \quad (\text{C47})$$

where we have reversed the order of integration over ϕ and \mathbf{r}_{\perp} , performed the $d-1$ integral over \mathbf{r}_{\perp} , and used the relation $\omega = 2 - d + \sigma$ in the second equality.

The remaining integral over ϕ in the resulting expression converges for all $\omega > -2$ and $d > 1$, and is tabulated[23]. This is readily seen to again recover (2) and (4), with the result given by

$$C(\sigma, d) = \frac{2\pi^{(d-1)/2} \Gamma(2 + \sigma) \Gamma(\frac{1}{2}(\omega + 2))}{a^{\omega} \Gamma(\frac{1}{2}(\sigma + 3))}, \quad (\text{C48})$$

where in the second equality we have again used (C32).

Surprisingly, although this expression looks quite different from (C33), it is, in fact, identical to it. To see this, we take the ratio of the expression (C48) for $C(\sigma, d)$ and the expression (C33) for it. Calling this ratio R , we find

$$R = \frac{2^{\omega}}{\omega\pi^{3/2}} \sin(\omega\pi) \Gamma(\frac{1}{2}(\omega + 2)) \Gamma(1 - \omega) \Gamma(\frac{1}{2}(\omega + 1)), \quad (\text{C49})$$

$$= \frac{1}{\omega\pi} \sin(\omega\pi) \Gamma(1 - \omega) \Gamma(\omega + 1), \quad (\text{C50})$$

$$= -\frac{1}{\pi} \sin(\omega\pi) \Gamma(-\omega) \Gamma(\omega + 1), \quad (\text{C51})$$

where we used the general identity for Gamma functions[23]

$$\Gamma(2x) = \frac{2^{2x-1}}{\sqrt{\pi}} \Gamma(x) \Gamma(x + 1/2) \quad (\text{C52})$$

with $x = \frac{1}{2}(2 + \sigma)$ and $x = \frac{1}{2}(1 + \omega)$,

$$\Gamma(2 + \sigma) = \frac{2^{\sigma+1}}{\sqrt{\pi}} \Gamma\left(\frac{2 + \sigma}{2}\right) \Gamma\left(\frac{3 + \sigma}{2}\right). \quad (\text{C53})$$

$$\Gamma(1 + \omega) = \frac{2^{\omega}}{\pi^{1/2}} \Gamma\left(\frac{1 + \omega}{2}\right) \Gamma\left(\frac{2 + \omega}{2}\right), \quad (\text{C54})$$

$\Gamma(1 - \omega) = -\omega\Gamma(-\omega)$, and the identity

$$\Gamma(1 - x)\Gamma(x) = \frac{\pi}{\sin(\pi x)} \quad (\text{C55})$$

with $x = 1 + \omega$, which reduces R to

$$R = -\left(\frac{\sin(\omega\pi)}{\pi}\right) \left(\frac{\pi}{\sin((\omega + 1)\pi)}\right) = 1. \quad (\text{C56})$$

This thereby proves that our expressions (C48) and (C33) are identical.

b. $\omega < -2$

For $\omega < -2$, the approach of the previous subsection does not work, since the integral over ϕ in Eq.(C47) does not converge.

We therefore take an alternative approach of calculating the integrals for the Fourier transform from real

space to Fourier space in Eq.(C39) by working in (hyper-) spherical coordinates. After taking $d - 2$ azimuthal angular integrals in (C39), we obtain

$$U_0(\mathbf{q}) = -\frac{K}{a^\omega} S_{d-1} \int_0^\infty dr r^{\sigma+1} \int_0^\pi \sin^{d-2} \theta e^{-iqr \cos \theta} . \quad (\text{C57})$$

Since we are restricting ourselves here to $\sigma > -2$ and $\omega < -2$, which implies $\sigma = d - 2 + \omega < d - 4$, we see that $-1 < 1 + \sigma < d - 3$. Hence, for $d \leq 4$, $-1 < 1 + \sigma < 0$. This is *precisely* the condition required to make the integral over r in (C57) converge in *both* the infra-red ($r \rightarrow \infty$; here the convergence is due in part to the oscillation of the complex exponential) and the ultra-violet ($r \rightarrow 0$). This constraint on the exponent $1 + \sigma$ also means we can close contours in the complex plane as in Fig.3(a) for $\cos \theta > 0$, and as in Fig.3(b) for $\cos \theta < 0$. This calculation is so similar to the one we did subsection (C1a) above that we will leave it to the reader to go through the details here, and simply note that the result is again Eq.(4), with now:

$$C(\sigma, d) = \frac{S_{d-1} \cos(\frac{1}{2}\sigma\pi) \Gamma(2 + \sigma) \Gamma(\frac{1}{2}(d - 1)) \Gamma(-\frac{1}{2}(1 + \sigma))}{a^\omega \Gamma(-\frac{1}{2}\omega)} . \quad (\text{C58})$$

Once again, although this expression looks very different from (C33), it is, in fact, identical to it. To see this, we take the ratio of the expression (C58) for $C(\sigma, d)$ and the expression (C48) for it (we proved earlier that (C48) is identical to (C33)). Calling this ratio R , we find

$$R = \frac{\cos(\frac{1}{2}\sigma\pi) \Gamma(-\frac{1}{2}(1 + \sigma)) \Gamma(\frac{1}{2}(3 + \sigma))}{\sin(\frac{1}{2}\omega\pi) \Gamma(\frac{1}{2}(1 + \omega)) \Gamma(\frac{1}{2}\omega)} . \quad (\text{C59})$$

Using equation (C55) in the numerator with $x = -(\frac{1+\sigma}{2})$ shows that the numerator of this expression is equal to $-\pi$. Likewise, using equation (C55) in the denominator with $x = -\frac{\omega}{2}$ shows that the denominator of this expression is also equal to $-\pi$. Hence, $R = 1$, proving that (C58) is identical to (C48), and, hence, to (C33).

c. $d = 1, -1 < \omega < 0$

For a variety of reasons (e.g., the absence of components \mathbf{r}_\perp of \mathbf{r} perpendicular to \mathbf{q}), the one-dimensional case has to be treated separately for $\omega < 0$. Fortunately, for $-1 < \omega < 0$, the necessary integrals to directly calculate $U_0(q)$ from $U_0(r)$ (note that both r and q are scalars in one dimension) can easily be done by the sort of complex contour techniques we have used above. We start with

$$\begin{aligned} U_0(q) &= -\frac{K}{a^\omega} \int_{-\infty}^\infty dr |r|^\omega e^{-iqr} , \\ &= -\frac{K}{a^\omega} \int_0^\infty dr r^\omega e^{iqr} + \text{complex conjugate} . \end{aligned} \quad (\text{C60})$$

For $-1 < \omega < 0$, the first integral on the second line converges at both small and large r , and can be evaluated by

rotating the contour as in Fig.3(b). Making the change of variable of integration from r to t via $r = it/q$ gives

$$\begin{aligned} U_0(q) &= -\frac{K}{a^\omega q^{\omega+1}} 2 \cos[(\omega + 1)\pi/2] \int_0^\infty dt t^\omega e^{-t} \\ &= -\frac{K}{a^\omega q^{2+\sigma}} 2 \cos[(\omega + 1)\pi/2] \Gamma(\omega + 1) . \end{aligned} \quad (\text{C61})$$

where in the second equality we have used $\omega = 2 - d + \sigma$ with $d = 1$. This recovers Eq. (4) of the Introduction, with

$$C(\sigma, d = 1) = 2 \sin(\omega\pi/2) \Gamma(\omega + 1) / a^\omega . \quad (\text{C63})$$

Once again, although this constant looks quite different from its expression in (C33), it is, in fact, identical to it, for $d = 1$ and $\omega = 1 + \sigma$.

d. Potentials that fall off faster than r^{-d}

Potentials that fall off faster than r^{-d} are qualitatively different from the cases just considered, since their volume integrals converge at large r . Thus the volume integral of such potentials is non-infinite, assuming that any short distance divergences are regularized, either by introducing a lattice, or having a regularized, integrable behavior of the potential at small r .

In contrast to the potentials with $\sigma > -2$ that we have been considering up to now, such potentials therefore, have Fourier transforms that remain *finite* as wavenumber $q \rightarrow 0$. The ‘‘Debye-Huckel screened’’ potentials treated in the main text have this property, as we’ll now show.

Here, we therefore consider the Fourier transform of a potential $U(\mathbf{r})$ which at large r falls off like

$$U(\mathbf{r}) \approx K_{DH} \left(\frac{a}{r}\right)^\gamma \quad (\text{C64})$$

with $\gamma > d$, and is integrable at small r .

As noted above, although such a potential has a *finite* Fourier transform $U(\mathbf{q})$ as $\mathbf{q} \rightarrow 0$, as we will now show, it always exhibits non-analyticity at sufficiently high order in q . To see this, we begin by noting that, due to the isotropy of the real space potential $U(\mathbf{r})$, the Fourier transform $U(\mathbf{q})$ is a function only of the *magnitude* q of \mathbf{q} . Defining this function via $U(\mathbf{q}) \equiv U(q)$, and differentiating the Fourier transform $U(\mathbf{q})$ of $U(\mathbf{r})$ with respect to q gives

$$\frac{dU}{dq} = -i K_{DH} a^\gamma S_{d-1} \int_0^\pi d\theta \sin^{d-2} \theta \cos \theta I(q \cos \theta) , \quad (\text{C65})$$

where we have defined

$$I(q \cos \theta) = \int_0^\infty dr r^{d-\gamma} e^{-iqr \cos \theta} \quad (\text{C66})$$

For γ in the range $d + 1 > \gamma > d$, the integral in this expression converges at non-zero q , but diverges as $q \rightarrow 0$.

We can extract that divergence by rotating the contour as in Fig. (3)(a) for $\cos \theta > 0$, and as in Fig. (3)(b) for $\cos \theta < 0$. Using those two results in (C65) gives

$$\begin{aligned} \frac{dU}{dq} &= -i \frac{K_{DH} a^\gamma S_{d-1} \Gamma(d - \gamma + 1)}{q^{d-\gamma+1}} \left[e^{-i\frac{1}{2}\pi(d-\gamma+1)} \int_0^{\pi/2} d\theta \sin^{d-2} \theta \cos^{\gamma-d} \theta \right. \\ &\quad \left. + e^{i\frac{1}{2}\pi(d-\gamma+1)} \int_{\pi/2}^\pi d\theta \sin^{d-2} \theta \cos \theta (-\cos \theta)^{\gamma-d-1} \right], \end{aligned} \quad (C67)$$

$$= -K_{DH} a^\gamma q^{\gamma-d-1} 2\pi^{(d-1)/2} \cos(\pi(\gamma-d)/2) \Gamma(d-\gamma+1) \Gamma\left(\frac{1}{2}(\gamma-d+1)\right) / \Gamma(\gamma/2), \quad (C68)$$

where to obtain the final equality, we substituted $\phi = \pi - \theta$ in the second integral to reduce it to the minus the first integral, which is tabulated. This result holds for $d + 1 > \gamma > d$.

To extend the Fourier transform result for values of γ to the range $d + n > \gamma > d + n - 1$, where n is an integer, we can proceed similarly by taking n derivatives of $U(q)$, which gives

$$\begin{aligned} \frac{d^n U}{dq^n} &= (-i)^n K_{DH} a^\gamma S_{d-1} \int_0^\pi d\theta \sin^{d-2} \theta \cos^n \theta \\ &\quad \times \int_0^\infty dr r^{d-\gamma-1+n} e^{-iqr \cos \theta}, \end{aligned} \quad (C69)$$

$$= (-1)^n K_{DH} a^\gamma q^{\gamma-d-n} 2\pi^{(d-1)/2} \cos(\pi(\gamma-d)/2) \Gamma(d-\gamma+n) \Gamma\left(\frac{1}{2}(\gamma-d+1)\right) / \Gamma(\gamma/2), \quad (C70)$$

where the integral over r converges by construction for all non-zero q , and diverges as $q \rightarrow 0$. Integrating this

expression n times, and making repeated use of the recursion relation for Gamma functions $\Gamma(x+1) = x\Gamma(x)$, we obtain

$$U(q) = \sum_{m=0}^{[n/2]} a_m q^{2m} + \frac{2\pi^{(d-1)/2} \cos(\pi(\gamma-d)/2) \Gamma(d-\gamma) \Gamma\left(\frac{1}{2}(\gamma-d+1)\right)}{\Gamma(\gamma/2)} K_{DH} a^\gamma q^{\gamma-d}, \quad (C71)$$

where the a_m 's are constants of integration characterizing the analytic part of $U(q)$, $[x]$ is the greatest integer function, and only even powers survive because all odd derivatives of $U(q)$ at $q = 0$ vanish, being proportional to integrals of odd powers of $\cos \theta$.

(39) for C_{DH} with

$$G(\sigma, d) = \frac{\Gamma\left(\frac{d+\sigma+2}{2}\right) \pi^{\frac{1-d}{2}}}{2\Gamma\left(\frac{3+\sigma}{2}\right) \cos\left(\frac{\sigma\pi}{2}\right) \Gamma(-2-\sigma)}. \quad (C72)$$

Plots of $G(\sigma, d)$ for $d = 1, 2$ and 3 are given in Figs (5), (6), and (7), respectively.

In section (IV A), we showed that the first non-analytic term in the expansion of the Fourier transform $U_{\text{eff}}(\mathbf{q})$ of the Debye-Huckel screened potential $U_{\text{eff}}(\mathbf{r})$ is $-\left(\frac{(k_B T)^2 \bar{K}}{g^2}\right) q^{2+\sigma}$. Comparing this with our result above implies that we must have $\gamma = d + 2 + \sigma$, which implies Eq.(7). Equating the coefficients gives our expression

The apparent singularities in (C72) at $\sigma = \pm 1$ are not, in fact, present, due to the cancellation of the divergences of $\Gamma(-2-\sigma)$ at those values of σ with the vanishing of the $\cos\left(\frac{\sigma\pi}{2}\right)$ factor. Taking the limit $\sigma \rightarrow \pm 1$ of (C72) carefully, with a little help from the Marquis de l'Hôpital, we find the perfectly finite results

$$G(\sigma = -1, d) = \frac{\Gamma\left(\frac{d+1}{2}\right)}{\pi^{\frac{d+1}{2}}}, \quad (C73)$$

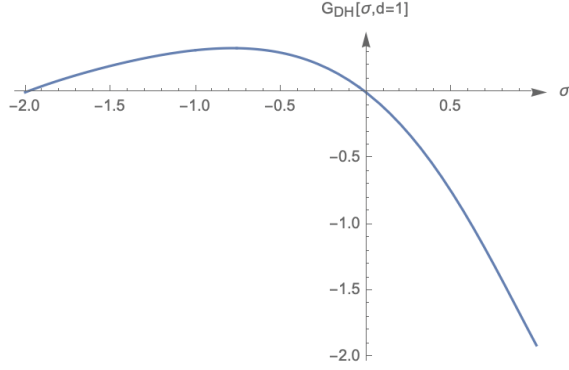


FIG. 5. Plot of $G(\sigma, d = 1)$ for the range of σ s accessible to our theory over which the potential can be Debye-Huckel screened, which is $-2 < \sigma < 1$.

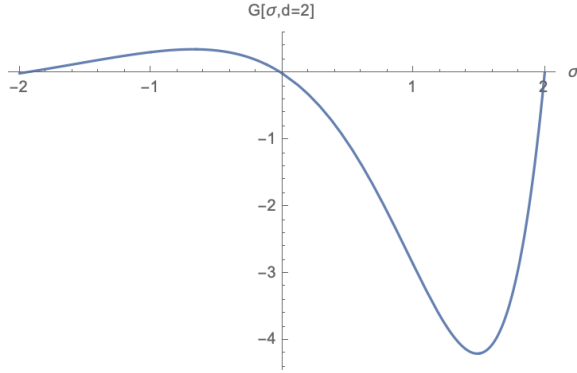


FIG. 6. Plot of $G(\sigma, d = 2)$ for the range of σ s accessible to our theory over which the potential can be Debye-Huckel screened, which is $-2 < \sigma < 2$.

and

$$G(\sigma = 1, d) = -\frac{6\Gamma\left(\frac{d+3}{2}\right)}{\pi^{\frac{d+1}{2}}}. \quad (\text{C74})$$

Indeed, $G(\sigma, d)$ is a perfectly smooth, non-singular function of σ for all three physical d 's, as can be seen from the plots of figures (5), (6), and (7).

Appendix D: Summary of long-range Ginzburg-Landau model results

In this Appendix we summarize the results of a complementary Ginzburg-Landau approach by Fisher, et al.[19], which treats the long-range interacting PM-FM transition from the paramagnetic side. Working in terms of the soft-spin order parameter $\psi = |\psi|e^{i\phi} = S_x + iS_y$,

$$H_{\text{Fisher}} = \frac{J}{2} \int_{\mathbf{q}} q^{2-\sigma} |\vec{S}_{\mathbf{q}}|^2 + u \int_{\mathbf{r}} (\vec{S} \cdot \vec{S})^2, \quad (\text{D1})$$

Fisher et. al.[19] have analyzed the transition in a long-ranged $O(n)$ model in d dimensions with power-law

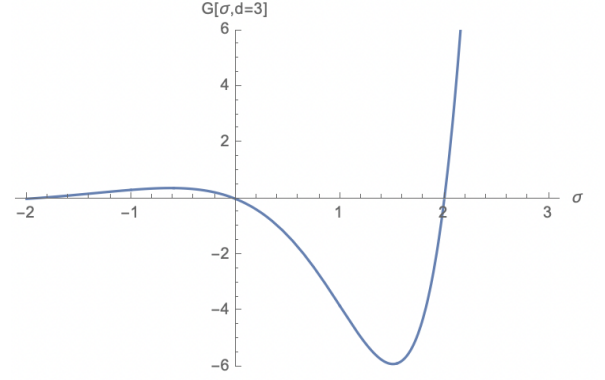


FIG. 7. Plot of $G(\sigma, d = 3)$ for the range of σ s accessible to our theory over which the potential can be Debye-Huckel screened, which is $-2 < \sigma < 3$.

exchange[20]

$$J_F(r) \sim \frac{1}{r^{d+\sigma_F}}, \quad (\text{D2})$$

where in terms of our exponent σ , their exponent $\sigma_F = 2 - \sigma$. Applying their results to the 2D XY model, we observe that the transition is clearly *not* of the Kosterlitz-Thouless type that one would expect were the screening of long-range exchange at play (it is *not*, as we argued in the main text) via the (failed) mapping onto screened super-Coulomb gas analyzed in the main text.

Indeed, Fisher et.al.'s work showed that in d -dimensions the transition is characterized by the conventional critical exponents η , ν , γ , α , and β , giving, respectively, the behavior of the spin-spin correlation function at the transition:

$$\langle \mathbf{S}_{\mathbf{r}} \cdot \mathbf{S}_{\mathbf{r}'} \rangle \propto |\mathbf{r} - \mathbf{r}'|^{2-d-\eta}, \quad (\text{D3})$$

the divergence to the spin-spin correlation length ξ , the magnetic susceptibility χ , and the specific heat C with temperature as the transition temperature T_c is approached:

$$\xi \propto |T - T_c|^{-\nu}, \quad \chi \propto |T - T_c|^{-\gamma}, \quad C \propto |T - T_c|^{-\alpha}, \quad (\text{D4})$$

and, last but not least, the vanishing of the magnetization $M \equiv |\langle \mathbf{S}_{\mathbf{r}} \rangle|$ with $T_c - T$ as the transition is approached from low temperature:

$$M \propto |T_c - T|^\beta. \quad (\text{D5})$$

Fisher et. al.[19, 20] found in $d = 2$:

$$\eta = 2 - \sigma, \quad \nu = \frac{1}{2 - \sigma}, \quad \beta = \frac{1}{2}, \quad \gamma = 1, \quad \alpha = \frac{2(1 - \sigma)}{2 - \sigma} \quad (\text{D6})$$

for $1 < \sigma < 2$ (the long-range analog of the mean-field

behavior), and

$$\begin{aligned}\eta &= 1 + \frac{\epsilon}{2} + O(\epsilon^2) , \quad \nu = 1 + \frac{2\epsilon}{5} + O(\epsilon^2) \\ \beta &= \frac{1}{2} + \frac{13\epsilon}{20} + O(\epsilon^2) , \quad \gamma = 1 + \frac{2\epsilon}{5} + O(\epsilon^2) , \\ \alpha &= -\frac{4\epsilon}{5} + O(\epsilon^2)\end{aligned}\tag{D7}$$

for $0 < \sigma < 1$, where $\epsilon \equiv 2(1 - \sigma)$.

For the borderline case of $\sigma = 1$ (which is relevant to the experiments of Chen, et. al.,[4]), one obtains universal logarithmic corrections:

$$\begin{aligned}\xi &\propto |T - T_c|^{-1} \left[\ln \left(\frac{T_c}{|T - T_c|} \right) \right]^{2/5} \propto \chi \\ M &\propto |T - T_c|^{1/2} \left[\ln \left(\frac{T_c}{|T - T_c|} \right) \right]^{3/10} , \quad C \propto \left[\ln \left(\frac{T_c}{|T - T_c|} \right) \right]^{-4/5} .\end{aligned}\tag{D8}$$

None of these is remotely like the Kosterlitz-Thouless transition, for which $\nu = \infty$ and $\alpha = -\infty$ [10]. Hence, the long-ranged XY model, despite the similarity of its single vortex energy to that of our super-Coulombic plasma, does *not* belong to the same universality class as the latter. In fact, it is clear that a simple screening picture of vortices in the long-ranged XY model fails.

Fortunately, such a picture is not needed, at least for σ between 1 and 2, or σ slightly less than 1, for which the above quoted results provide a complete picture. For σ well below 1, there is no analytic approach we know of to obtain the exponents. However, it seems exceedingly unlikely that the problem will ever map onto the screened Coulomb problem we have considered in this paper.

-
- [1] B. Yan, S. A. Moses, B. Gadway, J. P. Covey, K. R. A. Hazzard, A. M. Rey, D. S. Jin, and J. Ye, *Observation of dipolar spin-exchange interactions with lattice-confined polar molecules*, Nature 501, 521-525 (2013).
 - [2] L. Christakis, J. S. Rosenberg, R. Raj, S. Chi, A. Morningstar, D. A. Huse, Z. Z. Yan, and W. S. Bakr, *Probing site-resolved correlations in a spin system of ultracold molecules*, <https://arxiv.org/abs/2207.09328>.
 - [3] C. D. Bruzewicz, J. Chiaverini, R. McConnell, and J. M. Sage, *Trapped-ion quantum computing: Progress and challenges*, Applied Physics Reviews 6, 021314 (2019).
 - [4] C. Chen, G. Bornet, M. Bintz, G. Emperauger, L. Leclerc, V. S. Liu, P. Scholl, D. Barredo, J. Hauschild, S. Chatterjee, M. Schuler, A. M. Laeuchli, M. P. Zaletel, T. Lahaye, N. Y. Yao, and A. Browaeys, *Continuous Symmetry Breaking in a Two-dimensional Rydberg Array*, <https://arxiv.org/abs/2207.12930>.
 - [5] L. Radzihovsky, Q. Zhang, *Liquid crystal cells with "dirty" substrates*, Phys. Rev. Lett. 103, 167802 (2009).
 - [6] Q. Zhang and L. Radzihovsky, *Stability and distortions of liquid crystal order in a cell with a heterogeneous substrate*, Phys. Rev. E 81, 051701 (2010).
 - [7] Q. Zhang and L. Radzihovsky, *Smectic-glass transition in a liquid crystal cell with a "dirty" substrate*, Europhysics Letters 98, 56007 (2012).
 - [8] Q. Zhang and L. Radzihovsky, *Smectic order, pinning, and phase transition in a smectic liquid crystal cell with a random substrate*, Phys. Rev. E 87, 022509 (2013).
 - [9] Y. Pramudya, H. Terletska, S. Pankov, E. Manousakis, and V. Dobrosavljevic, *Nearly frozen Coulomb liquids*, Phys. Rev. B 84, 125120 (2011).
 - [10] J.M. Kosterlitz and D.J. Thouless, *Ordering, metastability and phase transitions in two-dimensional systems*, J. Phys. C: Solid State Phys. 6 1181 (1973).
 - [11] J. V. Jose, L. P. Kadanoff, S. Kirkpatrick, and D. R. Nelson, *Renormalization, vortices, and symmetry breaking perturbations in the two-dimensional planar model*, Phys. Rev. B 16, 1217 (1977).
 - [12] J. Villain, *Theory of one-dimensional and two-dimensional magnets with an easy magnetization plane. II. The planar, classical, two-dimensional magnet*, J. Phys. France 36, 581 (1975).
 - [13] See Appendices.
 - [14] For even integers, this expansion fails because the Fourier transform of even power of q is always a derivative of a delta function, and, hence, vanishes for non-zero \mathbf{r} . This vanishing is the result of the well-known exact cancellations that arise when one integrates the complex exponential $e^{i\mathbf{q}\cdot\mathbf{r}}$ over all \mathbf{r} . It does not occur once the complex exponential is multiplied by a non-even integer power of

- q .
- [15] The range of validity of this result is given in the Appendix[13].
- [16] R. M. Corless, G. H. Gonnet, D. E. G. Hare, D. J. Jeffrey, and D. E. Knuth, "On the Lambert W Function", *Advances in Computational Mathematics* **5**, 329 (1996).
- [17] J. M. Kosterlitz, *Phase Transitions in Long-Range Ferromagnetic Chains*, *Phys. Rev. Lett.* **37**, 1577 (1976).
- [18] A naive (i.e., incorrect) treatment of the long-range XY model in (58), transforms it into a harmonic model (63), allowing vortices. Dualizing this model using vortex form in (61) then seemingly transforms the power-law XY model to the power-law super/sub-Coulombic vortex gas, defined by H in (1) and (2). Such transformation would thus erroneously predict a screening of the long-range XY model (with exchange in (59) with $\sigma > 0$) to a conventional, short-range ($\sigma = 0$) XY model.
- [19] M. E. Fisher, S. K. Ma, and B. G. Nickel, *Critical exponents for Long-Range Interactions*, *Phys. Rev. Lett.* **29**, 917 (1972).
- [20] Reference [19] uses a different definition of σ , which we refer to as σ_F , defining the exchange interaction to be $J_{\mathbf{r},\mathbf{r}'} \propto \frac{J_0}{|\mathbf{r}-\mathbf{r}'|^{d+\sigma_F}}$. Comparing this with our definition (generalized to arbitrary spatial dimensions d) $\propto \frac{J_0}{|\mathbf{r}-\mathbf{r}'|^{d+2-\sigma}}$, we see that $\sigma_F = 2 - \sigma$, where σ_F is the definition used in [19], while σ is the definition we use here. All of the discussion in our paper is in terms of our definition of σ , obtained by the substitution $\sigma \rightarrow \sigma_F \equiv 2 - \sigma$ from the results of [19].
- [21] Guido Giachetti, Nicolo Defenu, Stefano Ruffo, Andrea Trombettoni, *Villain model with long-range couplings*, *Journal of High Energy Physics*, 2023(2), 1-25 (2022).
- [22] Igor F. Herbut, Babak H. Seradjeh, *Permanent confinement in the compact QED3 with fermionic matter*, *Phys. Rev. Lett.* **91**, 171601 (2003).
- [23] I. S. Gradshteyn and I. M. Ryzhik, *Table of Integrals, Series, and Products*, 4th edition, Academic Press, New York (1980). .